

THE DESIGN OF A SURFACE LAUNCH AND
RECOVERY FENDER FOR DSRV 'ALVIN'

by

JAMES FRANCIS O'SULLIVAN, JR.

B.S.M.E., North Carolina State University
(1971)

SUBMITTED IN PARTIAL FULFILLMENT OF THE
REQUIREMENTS FOR THE DEGREE OF
OCEAN ENGINEER

at the

MASSACHUSETTS INSTITUTE OF TECHNOLOGY

and the

WOODS HOLE OCEANOGRAPHIC INSTITUTION

and

MASTER OF SCIENCE IN OCEAN ENGINEERING

at the

MASSACHUSETTS INSTITUTE OF TECHNOLOGY

September, 1973

Signature of Author .

Joint Program in Ocean Engineer-
ing, Massachusetts Institute of
Technology - Woods Hole Oceano-
graphic Institution, and Depart-
ment of Ocean Engineering,
Massachusetts Institute of
Technology, September 1973

Certified by

~~Thesis Supervisor~~

Certified by

Thesis ~~S~~ Supervisor

Accepted by .

Chairman, Joint Committee for Ocean Engi-
neering Massachusetts Institute of Tech-
nology - Woods Hole Oceanographic Insti-
tution

WHOI-1786

GC
7.6
080
1973

ABSTRACT

Surface recovery of small submersibles could be made safer for personnel and hardware with the installation on the submersible of an inflatable, pneumatic bumper which acts also as main surface buoyancy. The use of such a bumper in the recovery of DSRV ALVIN by her catamaran mother ship, LULU, is the subject of this study. It was determined, from first order analysis of the surge velocities of these two vessels in recovery position in a sea state 6, that any such bumper or combination of bumpers (i.e. bumper on LULU) would have to absorb 10,000 ft.-lb_f. of energy. In order to protect the mechanical arm, keep the forces of collision at an acceptable level and retain present surface buoyancy, an increase in ascent and descent time must be tolerated since the uninflated vertical projected area of the forebody must increase. Large trim moments, due to the presence of the air bumper at the bow, can be eliminated by use of a partially submerged bumper.

ACKNOWLEDGEMENTS

This study was accomplished with the advice and assistance of many people. I would like to thank, in particular, the following persons: Jim Mavor and M.A. Abkowitz for their continuous assistance as thesis advisors; William O. Rainnie, Larry Shumaker and all the members of the W.H.O.I. Deep Submergence Group; Neil Brown for the use of his computer; Allyn C. Vine for his timely suggestions; and a special thanks to my sisters, Eileen and Peggy, for their encouragement and patience during the final preparation of this thesis.

TABLE OF CONTENTS

Abstract	i
Acknowledgements	ii
Notation	iv
Chapter 1: Introduction	1
Background	1
Intermediate Vehicle	8
Removal of Pontoon Curvature and Attachment of Bumper to ALVIN	12
Chapter 2: Analysis	18
Introduction	18
Surge Velocity Analysis	21
Energy Analysis	34
Bumper Geometric Analysis	38
Chapter 3: Results	46
Surge Velocities and Energy of Collision	46
Geometric Analysis of Bumper	47
Chapter 4: Discussion	61
Chapter 5: Conclusions	69
Bibliography	71

NOTATION

A	wetted cross-sectional area of pontoons
a_{ij}	added mass coefficients
a_0	$\frac{1}{2}$ bumper width
b_0	$\frac{1}{2}$ bumper depth
b_{ij}	linear drag coefficients
C_D	drag coefficient
c_{ij}	static restoring force coefficients
d	penetration depth
E_S	spring energy
E_T	total energy
F_A	forcing function of ALVIN
F_L	forcing function of LULU
F_{spring}	spring force
g	gravity
H	wave height
$H^{1/3}$	average 1/3 highest wave height
K	wave number
$K_{0,1,2,\dots}$	spring coefficients
L_m	mean bumper length
ℓ	ship length
M_A	mass of ALVIN
M_A'	virtual mass of ALVIN

NOTATION

A	wetted cross-sectional area of pontoons
a_{ij}	added mass coefficients
a_o	$\frac{1}{2}$ bumper width
b_o	$\frac{1}{2}$ bumper depth
b_{ij}	linear drag coefficients
C_D	drag coefficient
c_{ij}	static restoring force coefficients
d	penetration depth
E_s	spring energy
E_T	total energy
F_A	forcing function of ALVIN
F_L	forcing function of LULU
F_{spring}	spring force
g	gravity
H	wave height
$H^{1/3}$	average 1/3 highest wave height
K	wave number
$K_{0,1,2,\dots}$	spring coefficients
L_m	mean bumper length
l	ship length
M_A	mass of ALVIN
M_A'	virtual mass of ALVIN

M_L	mass of LULU
M_L'	virtual mass of LULU
Mom_T	total momentum
P	pressure
R	uninflated radius
R_p	protection radius
S	wetted area
T	wave period
t	time
V_A	velocity of ALVIN
\dot{V}_A	acceleration of ALVIN
V_L	velocity of LULU
\dot{V}_L	acceleration of LULU
V_3	velocity after collision
x	horizontal axis
X_A	response function for ALVIN
X_L	response function for LULU
z	vertical axis
β_A	ratio of drag to inertia, ALVIN
β_L	ratio of drag to inertia, LULU
γ	isentropic gas constant
ρ	density of water
λ	wave length
ϕ	velocity potential of wave

ϕ_0 total bumper angle effected by collision
 δ elemental displacement
 ω wave radial frequency

CHAPTER 1

INTRODUCTION

Background

The Deep Submergence Research Vehicle (DSRV) ALVIN (figure 1-1) and mother ship LULU (figure 1-2) function as one of the most unique and valuable oceanographic instruments available to scientific investigation of the benthic environment. The submersible and her mother ship are owned by the U.S. Navy and are operated by the Woods Hole Oceanographic Institution. They form a most successful combination, having completed over 400 dives from 1964 to 1972.

ALVIN displaces 15 long tons with an overall length of 22 feet, a beam of 8 feet and a height of $7\frac{1}{2}$ feet from skids to main deck. She is designed primarily for benthic operation with no specifically designed features for surface launch and recovery at sea except for tow line pads and twin docking keels.

LULU is a catamaran that displaces 437 long tons with an overall length of 100 feet, overall beam of 48 feet and an individual pontoon beam of 14 feet. Figure 1-3 shows the positioning of ALVIN and LULU for surface recovery. Shown also are some of the problems involved in docking ALVIN and LULU.

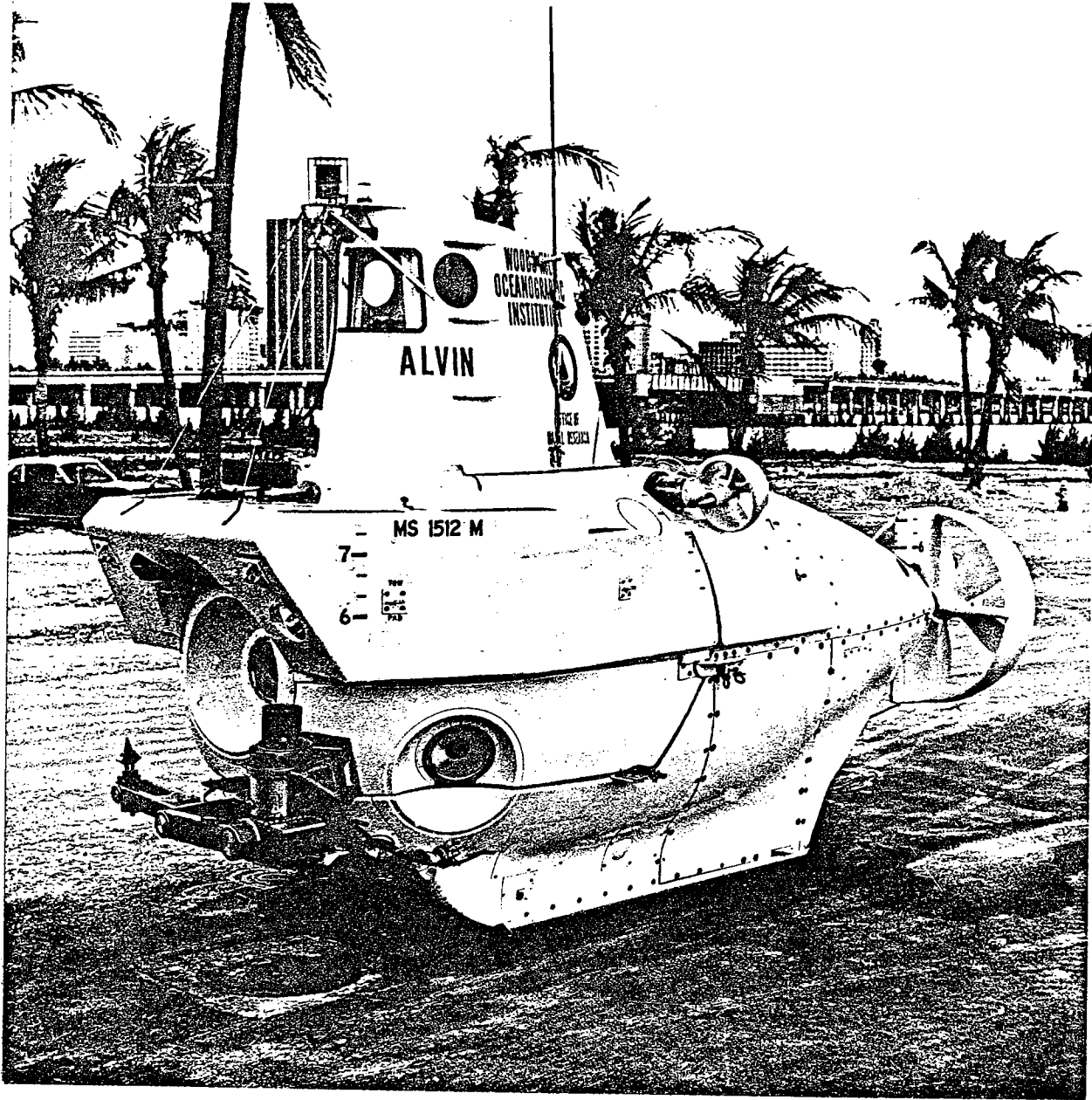


Figure 1-1. DSRV ALVIN.

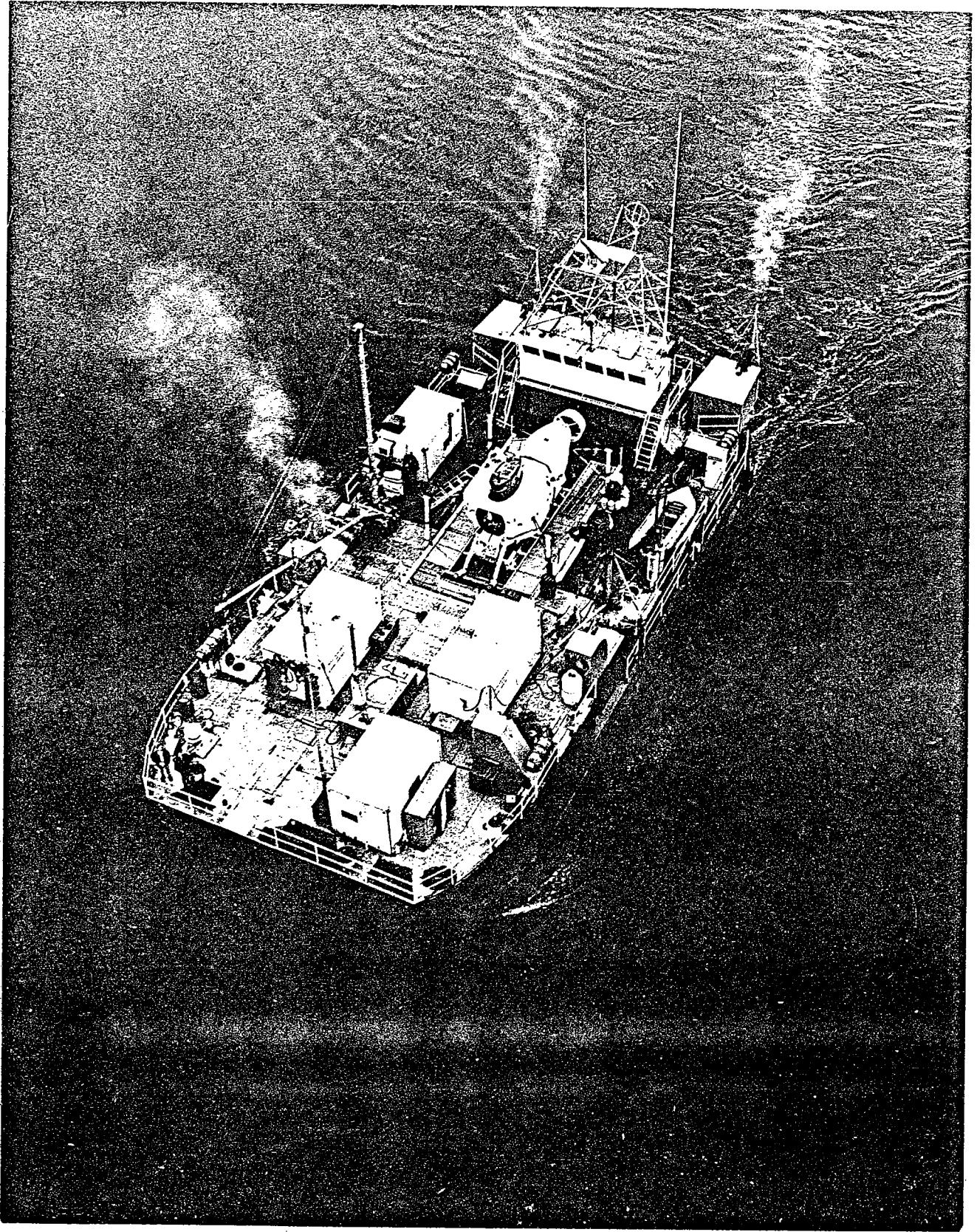


Figure 1-2. DSRVT LULU Underway with DSRV TURTLE.

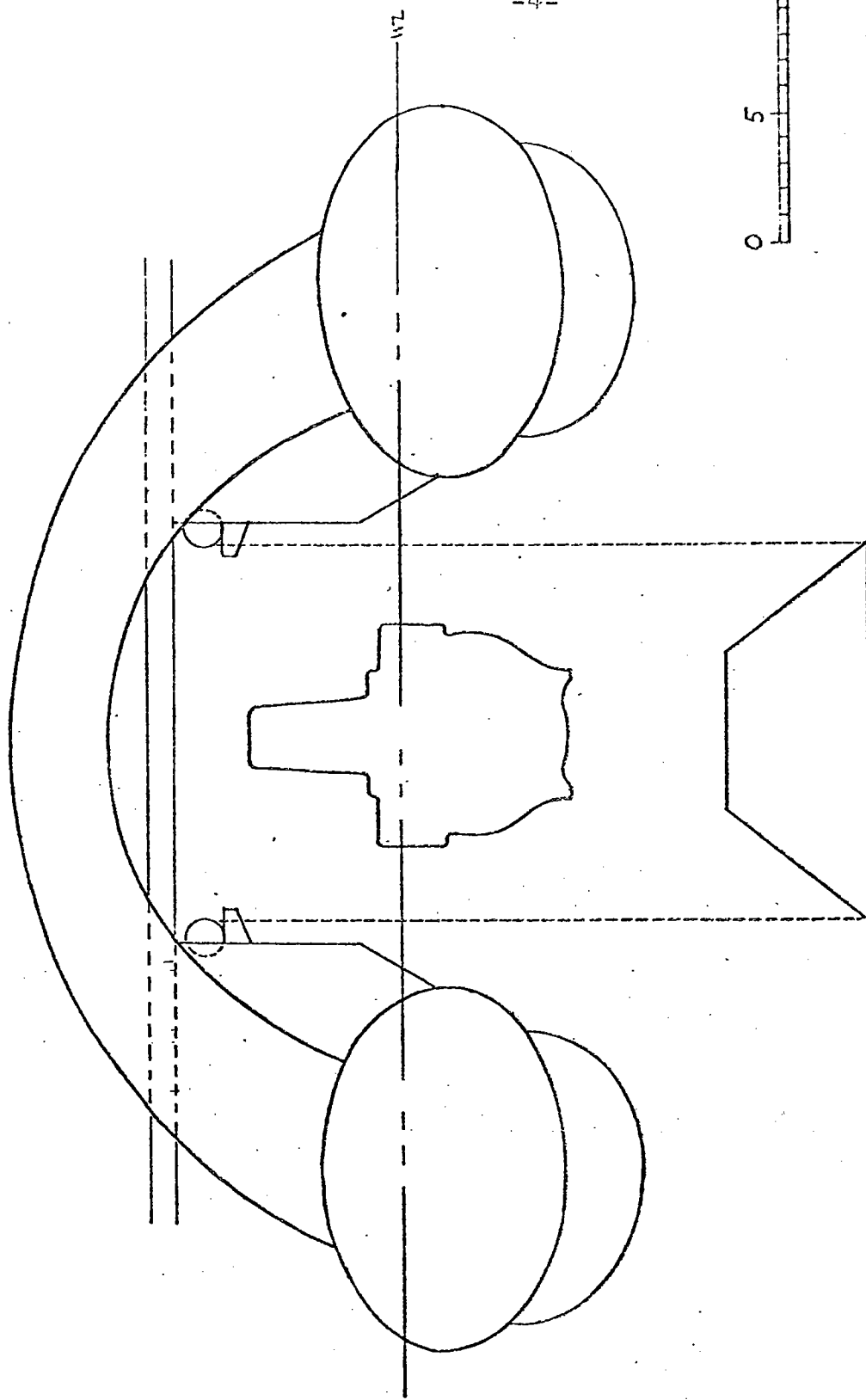


Figure 1-3. ALVIN Between Pontoons of LULU with Cradle in Recovery Position.

Notice the curvature of the ends of LULU's pontoons and the aft arch under which ALVIN must pass before mating with the cradle. Notice, too, the amount of space available for lateral motion between the pontoons and ALVIN. The cradle shown has a lifting capacity of 30 tons. It is supported at each of four points by one inch chain that runs through wild cats located just aft of midship.

Presently, docking is accomplished by having LULU close-in on the surfaced ALVIN and then maneuvering herself so that the seas are from astern. ALVIN approaches from the rear and swimmers enter the water to attach snubber lines to her towing pads. Line handlers standing on the pontoons guide ALVIN between the pontoons, under the arch and position her over the cradle, continuously preventing lateral collision between the sub and the pontoons. The cradle is raised at a rate of 30 feet per minute until it is clear of the air-water interface. The final raised position has the upper level of the cradle flush with the surrounding deck, thus allowing easy access to ALVIN. The cradle is two-blocked in this transit position. Launch is basically a reversal of this procedure.

This recovery scheme is limited to sea state 3 or less; therefore ALVIN's operating season is greatly reduced, with costly and time-consuming postponements necessary during operating cruises.

An alternate underwater recovery method was considered. This recovery scheme calls for the cradle to be lowered 100 feet below the surface. At this depth, ALVIN would no longer be under the influence of the wave action from a sea state 4. ALVIN would dock with the cradle and then be lifted up rapidly through the air-sea interface.

Towards this end, Vandiver (1969) conducted a study of the dynamics of a non-linearly damped spring-mass system such as would be the situation of ALVIN docked on the cradle at 100 feet below the surface. Following this was the modeling work of Cohen (1972) who used a 1/40 scale model of LULU with the cradle suspended 100 feet below. He ran this model in a wave tank, using sea state 4 conditions. His conclusion was: with the present recovery configuration, submerged recovery is not any more attractive than the present surface recovery because the present hoist system does not sufficiently decouple the surface motions of LULU from the cradle.

Proposals to decouple the motions of LULU from the cradle called for extensive and costly modifications to the present system. Subsequently, in January of 1973, William Rainnie, the Manager of Deep Submergence Operations, suggested that this author investigate possible schemes which would allow surface recovery in sea state 4 and higher. The two factors limiting present retrieval to sea state 3 were given as:

- (1) Personnel Safety - This includes the safety of the swimmers who must enter the water and attach the snubber lines to ALVIN and the line handlers who must stand on the pontoons during recovery. In sea state 4 or higher, it is possible for a man standing on the stern portion of the pontoons to be totally submerged when LULU pitches in head or following seas.
- (2) Submersible Safety - As mentioned earlier, ALVIN was designed for benthic operation and has no means of protecting herself or instruments attached to her exterior in case of collision with LULU during recovery. Many vital and costly pieces of

equipment and scientific samples have been lost during recovery in rough seas.

Intermediate Vehicle

The first approach investigated was suggested by Rainnie. It called for the use of an intermediate vehicle (tethered or untethered) which would go aft of LULU and dock with ALVIN, preferably without the help of swimmers. ALVIN, protected by the intermediate vehicle, could be pulled between the pontoons and into hoisting positions without the use of line handlers standing aft of the arch on the pontoons. The major advantage of this scheme was that it would call for minimum alterations to ALVIN and LULU. Accordingly, the major difficulty was that the intermediate vehicle had to be designed around the existing system. The design problems encountered were:

- (1) Docking With ALVIN - Aside from the obvious problem of matching the intermediate vehicle's wave response (RAO - Response Amplitude Operator) to ALVIN's wave response, there was the problem of where to dock. Docking from the front allowed for the chance of damaging or losing exterior instruments on ALVIN's bow.

Docking from the rear, as would be possible with an untethered vehicle, allowed for the chance of damaging the prop and shroud and thus crippling ALVIN. Since the strongest point on ALVIN's exterior is located near her center of gravity at midship, the most logical docking approach would be from the side. If ALVIN were eventually to dock with a single hull mother ship that required protection on only one side, this approach would be feasible. But in the case of docking with the interior of a catamaran, both sides and the bow must be protected.

- (2) Docking With LULU - Figure 1-3 shows one of the major docking problems with LULU, the curvature of the pontoons. Also, aft of the high arch, the pontoons are tapered so that the waterplane is reduced rapidly. Both of these factors pose the problem of the intermediate vehicle, with ALVIN connected, being caught under the pontoon. Cohen (1972) showed that the aft tip of the pontoons pitch up to 14 feet (above

and below mean sea level) in 9 foot seas with wave lengths of 160 feet (sea state 4). This calls for a high outer wall on the intermediate vehicle. From figure 1-3, it can be seen that the intermediate vehicle should have a 20 foot beam in order to prevent any lateral motion while between the pontoons. It can also be seen in this figure that the intermediate vehicle must retract its overall beam to not more than $13\frac{1}{2}$ feet in order to pass between the chains supporting the cradle. With ALVIN having an 8 foot beam, this leaves the intermediate vehicle with sides of only $2\frac{1}{2}$ feet in the retracted position.

- (3) Storage On LULU - There are serious storage space and weight limitations on LULU. The intermediate vehicle could not be stored on the deck level due to lack of space. The only available storage location for a vehicle of the size suggested already would be the area below the main deck and between the forward arch and the cradle well. This imposes a length limit of 30

feet. If the vehicle extends below the forward arch, a height of about 4 feet, it will take tremendous pounding in heavy seas. It has been shown that the vehicle's sides must be higher than 4 feet in order to accommodate the curvature of the pontoons. With the intermediate vehicle's storage area being separate from ALVIN's storage area on the main deck, there must be an uncoupling of the two vehicles while they still remain in the water and between the pontoons. Such an operation in heavy seas may prove to be no less dangerous to personnel and equipment than the present recovery operation. The conclusion for this approach was that the intermediate vehicle would be too massive and complex to be reliably operated as a necessary link in surface recovery. The initial requirement for designing around existing features in the present system led to the massive and complex design. The second approach followed the opposite point of view: modify LULU and ALVIN so that a

high sea state recovery could be accomplished without jeopardizing personnel or instrument safety and without the need of introducing a new vehicle into the system.

Removal of Pontoon Curvature and Attachment of Bumper to ALVIN

As the above heading indicates, the modifications being considered are the flattening of the interior walls and stern of LULU'S pontoons and the permanent attachment of a bumper to ALVIN. This bumper would protect instruments attached to the exterior of ALVIN during collision with LULU.

The curvature could be removed from the pontoons in one of several ways. It could be removed permanently by welding a flat plate to the interior of the pontoons, filling the gap between the pontoon and plate with buoyancy material. This would compensate for the weight of the plate. The curvature could be temporarily removed by the inflation of a water bumper below the waterline on the interior of the pontoons. This would give some resiliency to LULU during collision with ALVIN.

There are other possible schemes that could be investigated to remove the curvature, but the atten-

tion of this paper will now be concentrated on the second modification mentioned above: the attachment of a permanent bumper on ALVIN.

The possibility of combining main surface buoyancy with an inflatable bumper has been suggested in the past. Since the present main surface buoyancy of 1500 lb_f. is obtained by the discharge of air from the main buoyancy air tanks (2 tanks 23' I.D. at 2500 psi.) into an enclosed floodable compartment in the forebody, the proposed idea would use this air reserve to inflate the bumper which in turn would supply the main surface freeboard buoyancy. The design constraints to be considered for the bumper are:

- (1) Drag - The bumper should not appreciably increase drag in the horizontal or the vertical. Horizontal drag increases will decrease forward speed. But, more important, vertical drag increases will increase ascent and descent time by decreasing the ascent and descent terminal velocities.
- (2) Main Buoyancy - The present main surface buoyancy of ALVIN is 1500 lb_f. Without modifications to her present ballasting,

this parameter should be preserved.

- (3) Collision Force - For safety reasons, ALVIN's fore and afterbodies are at the present mechanically connected only at the base of the personnel sphere. Consequently, the force of collision transmitted by the bumper to the forebody should be minimized.
- (4) Trim Moment - Some increase in trim moment due to the inflation of the bumper at the bow can be compensated for by adjustment of the present ballast, but trim moment should be minimized.

The basic bumper geometry that was considered in this report is shown in figure 1-4. The plan view shows the uninflated perimeter as a solid line and the inflated perimeter as a broken line. The uninflated perimeter shown is waterline 4 expanded by $\frac{1}{2}$ bumper width, a_0 . Hence, the inflated perimeter shown is that of waterline 4 expanded by $3a_0$.

The sectional view of figure 1-4 further clarifies this. Again, the inflated bumper is shown by broken lines with the forebody shown by the cross-hatched area. Waterline 4 is retained up to main

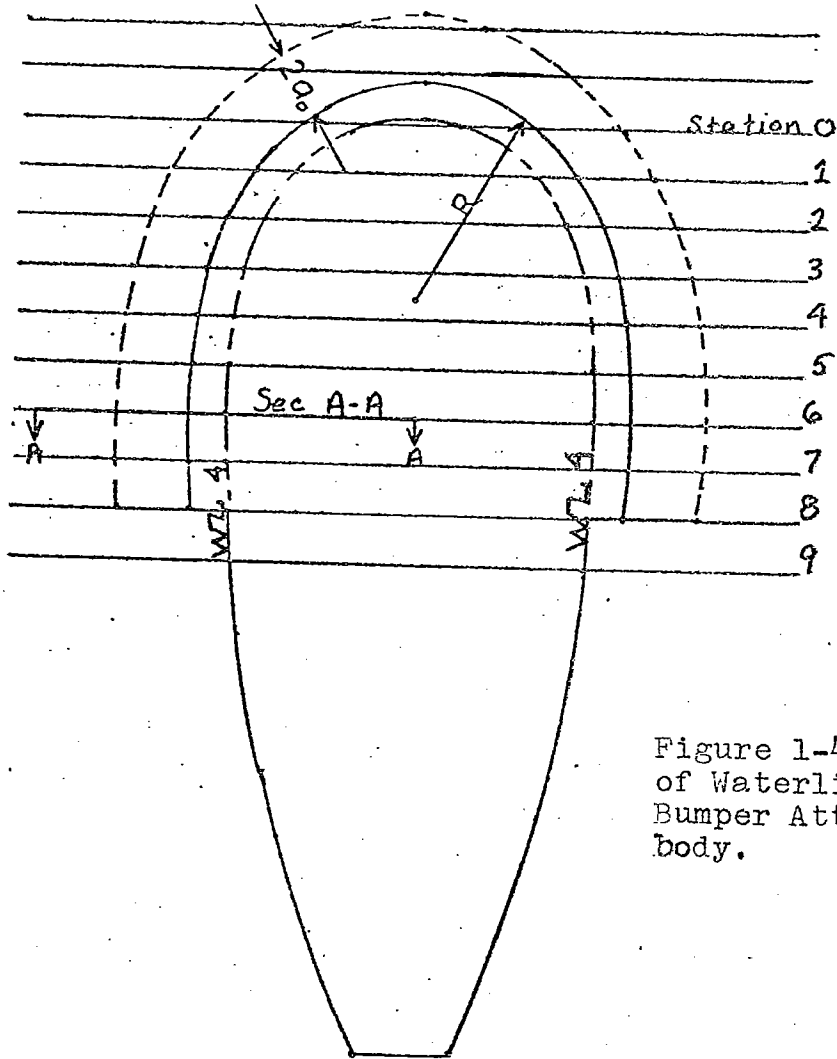
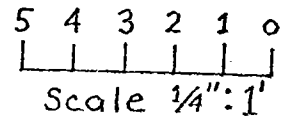
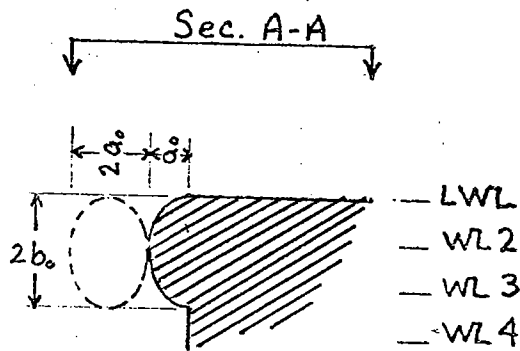


Figure 1-4. Plan View of Waterline 4 with Bumper Attached to Forebody.



deck level with a semi-elliptical lip (width = a_0) attached around the upper portion. This volume is made of syntactic foam.

The bumper itself is made of neoprene with dacron chord interior backing (to prevent stretch). The outer half of the bumper has a polyurethane plastic exterior surface. This is so that upon deflation, the inner half of the bumper will reverse curvature and conform with the outer half. This allows the whole bumper to seat snugly against the semi-elliptical lip on the forebody upon deflation. The uninflated form will have no sharp edges and will retain a horizontal and vertical projected area comparable to the present configuration. Therefore this scheme maximizes the inflated perimeter (hence increases protection) while minimizing increases in drag.

Other factors concerned with the bumper operation are:

- (1) The air release valves are located on the top of the bumper to allow complete air escape upon deflation.
- (2) The semi-rigid outer half of the bumper is spring loaded with the forebody so that

conformity is assured upon deflation.

- (3) Expansion sections must be included in the bumper where bumper surface area will need to increase upon inflation due to curvature.
- (4) Hoses connecting the bumper to the main air tanks in the afterbody must have pull-free connectors in case of emergency separation of the fore and afterbodies.

Waterline \mathcal{L} is semi-circular about the bow, centered at the intersection station 3.5 and the center line. The uninflated radius about the bow is R (see figure 1-4). Hence, the inflated radius will be equal to $R + 2a_0$. Note that the bumper in figure 1-4 extends to station 8 (the limit of the forebody). These geometric variables, along with $\frac{1}{2}$ bumper depth b_0 , are the quantities that must be varied so as to give the required results.

CHAPTER 2

ANALYSIS

Introduction

The bumper design requires investigation of the following areas:

- (1) The kinetic energy which a bumper would be required to absorb during collision between ALVIN and LULU.
- (2) The regions protected on ALVIN considering the above mentioned collision energy and various bumper geometries.

The first analysis requires the determination of the velocities of both vessels at the ocean surface. Here, assumptions will have to be made regarding the recovery positions of the vessels. As shown in figure 2-1, both vessels will be in head seas at zero forward vessel velocity. In order to maximize the phase difference between the responses of LULU and ALVIN to the waves, ALVIN will be aligned directly astern of LULU. With this alignment, the surface velocity components of interest will be the surge of both vessels. Determination of surge velocity for both vessels can be made

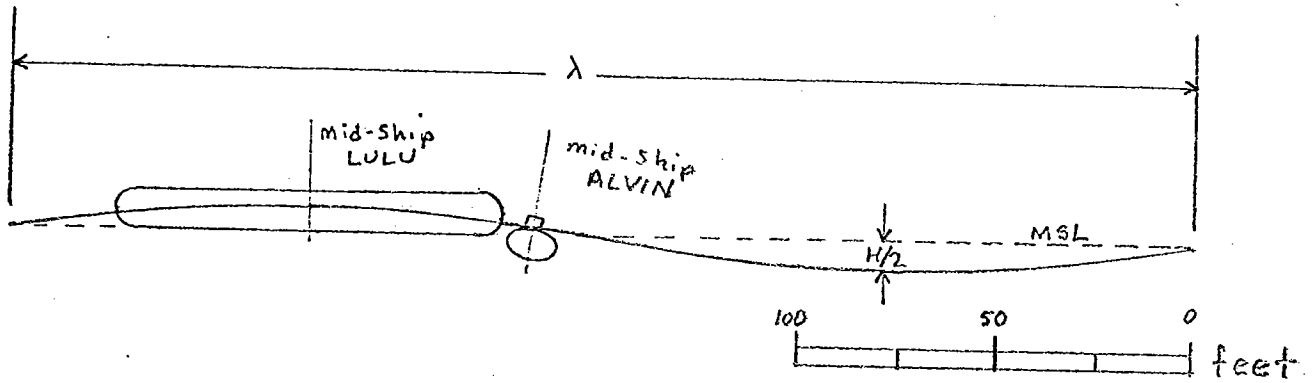


Figure 2-2. LULU and ALVIN in Recovery Position ($\lambda = 300$ feet, $H = 15$ feet).

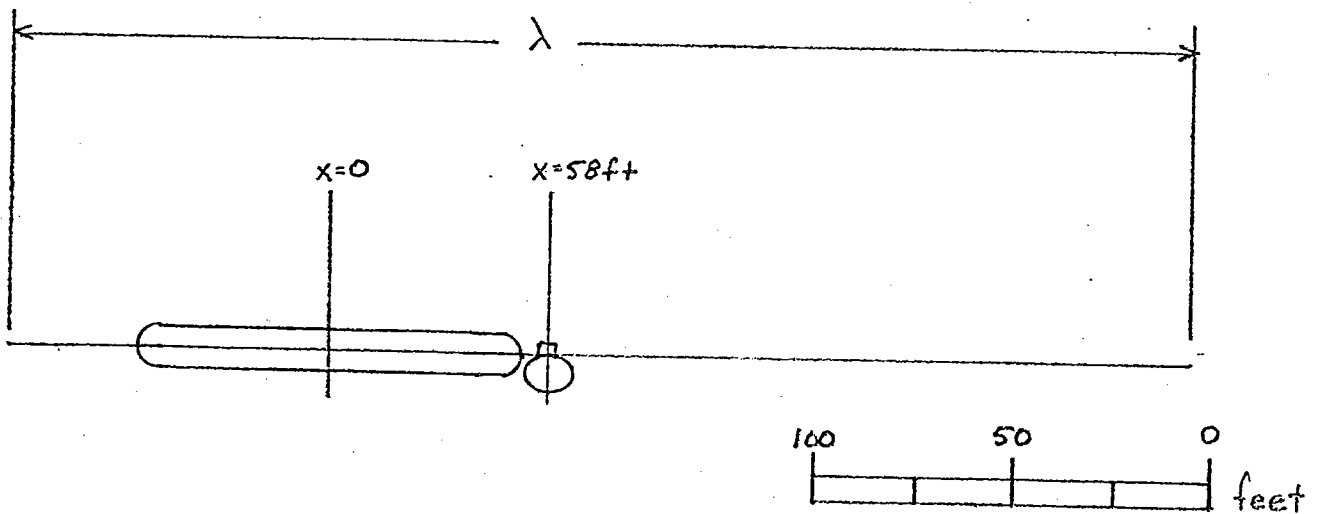


Figure 2-2. Linearized First Order Model of LULU and Alvin in Recovery Position.

by model test in a towing tank or by mathematical modeling. Since an approximate, conservative value for collision energy is sufficient, the latter approach will be followed.

The second area of investigation requires determining the volume change of the bumper caused by collision and the resulting protection perimeter on ALVIN. The total air reserve in the two main ballast tanks can be used to inflate the bumper. Hence, by considering isentropic change from ballast tank to bumper, the initial bumper volume and pressure are known for a given bumper geometry. The necessary volume change of the bumper required to absorb the collision energy can also be determined by assuming isentropic conditions.

The volume change caused by geometrically altering the bumper shape, as occurs in a collision, will be determined by numerical integration. This determination will give the protection perimeter as a function of volume change and bumper geometry. Comparison of the necessary volume change for energy absorption and the volume change for various protection perimeters is then possible.

Surge Velocity Analysis

First order theory for motions of bodies in a seaway equates the wave's exciting force on a rigid body to the response function of an oscillating body in still water. The "Froude-Krylov" exciting force approximation assumes that the pressure on the vessel's wetted surface area is a function of the wave's undistorted potential field only. This approximation is good for long, thin vessels that are small compared to the wave length.

Two points concerning the use of this exciting force approximation are made. First, LULU has two parallel pontoons each of which would affect the other's hydrodynamic behavior by establishing its own potential field. In surge, at low velocities (of the order of particle velocity), this effect would be small and will be neglected. Hence, hydrodynamic analysis will be done assuming an equivalent single pontoon.

Secondly, the stern of LULU acts as a wave generator when LULU is heaving and pitching. The wave system generated tends to propagate only away from LULU. Such a system would decrease ALVIN'S surge velocities toward LULU in the proximity of the stern.

Neglecting this effect would increase the collision energy and, hence, would be a conservative assumption.

Figure 2-2 shows the first order model of the system. Note the phase difference between LULU and ALVIN.

The expression for the pressure in a wave comes from Bernoulli's equation:

equation 2-1

$$p = -\rho \frac{\partial \phi}{\partial t} + \frac{1}{2} \rho V^2 + \rho g z$$

The last term is hydrostatic pressure and can be neglected in the determination of the horizontal exciting force. The middle term is the dynamic component which will be second order compared with the first term (and will be neglected). The first term represents the time rate of change of the velocity potential field, ϕ . The simple harmonic wave expression for ϕ is:

equation 2-2

$$\phi = \left(\frac{Hg}{2\omega} \right) e^{-kz} \cos(Kx - \omega t)$$

where: H = wave height

ω = wave frequency

K = wave number

Hence, pressure becomes:

equation 2-3

$$p = -\rho \frac{\partial \phi}{\partial t} = (\rho H g / 2) e^{-kz} \sin(kx - \omega t)$$

For near surface applications, $z \approx 0$:

equation 2-4

$$p = (\rho H g / 2) \sin(kx - \omega t)$$

The exciting force is the integral of equation 2-4 over the wetted surface area:

equation 2-5

$$F_x = - \int_{\text{wetted area}} p dA_x$$

Since LULU'S pontoons have constant cross-section except for their tapered bow and stern, equation 2-5 may be approximated by:

equation 2-6

$$F_L = A P_{\text{bow}} - A P_{\text{stern}}$$

where the first term refers to the pressure at the mid-point of the bow nose acting over the projected wetted surface area and the second term refers to the corresponding pressure at the stern. Recall

from figure 2-2 that the origin is at LULU's mid-ship section; the distance to the bow nose mid-point is - 40 feet and to the stern nose mid-point is + 40 feet. If 50 square feet (Kenny '69) is used as the wetted cross-sectional area, the expression for LULU'S exciting force becomes, with use of equation 2-4;

equation 2-7

$$F_L = \frac{\rho H g (50 \text{ ft}^2)}{2} [\sin(-40k - \omega t) - \sin(40k - \omega t)]$$

For deep water waves:

equation 2-8

$$\omega = 2\pi/T$$

equation 2-9

$$k = \omega^2/g = 4\pi^2/gT^2$$

where: T = wave period.

With $(\rho g)_{\text{water}} = 64 \text{ lb}_f/\text{ft}^3$, and using equations 2-8 and 2-9, equation 2-7 becomes, after trigometric manipulation:

equation 2-10

$$F_L = -3.22 \times 10^3 H \sin(49/T^2) \cos(-2\pi t/T)$$

In the case of ALVIN, the following application of Gauss's Theorem will be used:

equation 2-11

$$F_x = \oint_A p dA_x = \int_V \frac{\partial p}{\partial x} dV.$$

The pressure gradient in the x direction is obtained by differentiating equation 2-4 with respect to x:

equation 2-12

$$\frac{\partial p}{\partial x} = (2H\pi^2\rho/T^2) \cos\left(\frac{4\pi^2x}{gT^2} - \frac{2\pi t}{T}\right).$$

Again, equations 2-3 and 2-9 were used.

When $\sin \pi (l/\lambda) \approx \pi (l/\lambda)$, (λ being the wave length and l being the ship length), the pressure gradient may be approximated as a constant about midship. Equation 2-11 is then written as:

equation 2-13

$$F_A = - \left(\frac{M_A'}{\rho} \right) \left[(2H\pi^2\rho/T^2) \cos\left(\frac{4\pi^2x}{T^2} - \frac{2\pi t}{T}\right) \right].$$

The first term is the virtual displacement where M_A' is the virtual mass of ALVIN (the true mass plus the entrained mass of water). Entrained or added mass for bodies on or near a free surface

vary with wave frequency. But the added mass of a long, thin body in surge is only about 10% of its true mass. Hence, use of the deeply submerged added mass of a body will introduce only slight error in the value of virtual mass.

If ALVIN is modeled as a submerged spheroid with a length of 20 feet and true displacement of 15 long tons, a width and depth of 7 feet is obtained. The added mass in surge for this deeply submerged spheroid is 13% of true mass (Newman '71). Hence, equation 2-13 becomes:

$$F_A = (1.13) (15 \text{ L.tons}) \left(2240 \frac{\text{lb}_m}{\text{L.ton}} \right) \left(32.2 \frac{\text{lb}_f \cdot \text{s}^2}{\text{lb}_m \cdot \text{ft}} \right) \left(\frac{2H\pi^2}{T^2} \right) \cos \left(\frac{4\pi^2 x}{gT^2} - \frac{2\pi t}{T} \right)$$

equation 2-14

$$F_A = -2.34 \times 10^4 \left(\frac{H}{T^2} \right) \cos \left(\frac{4\pi^2 x}{gT^2} - \frac{6.28t}{T} \right)$$

The phase lag distance is the distance between midship LULU (the origin) and midship

ALVIN (figure 2-2). This is the sum of one-half of the length of each vessel or 58 feet since LULU is 96 feet long and ALVIN is 20 feet long. The final expression for the forcing function on ALVIN is given by:

equation 2-15

$$F_A = -2.34 \times 10^4 \left(H/T^2 \right) \cos \left(\frac{71}{T^2} - \frac{6.28t}{T} \right)$$

The general linear first order response function for a body in a wave system is given by:

equation 2-16

$$X_j(t) = \sum_{i=1}^6 (m_{ij} + a_{ij}) \ddot{\xi}_i(t) + b_{ij} \dot{\xi}_i(t) + c_{ij} \xi_i(t)$$

The j index denotes the response mode (surge, sway, heave, pitch, roll or yaw). The right hand side

terms are summed over the 6 modes. For symmetrically submerged bodies, the $i \neq j$ terms will be zero. The m_{ij} term is the true mass or mass moment of the body. The a_{ij} terms are the added mass coefficients. The b_{ij} terms are the hydrodynamic response that is in phase with the velocity. This is a low velocity linearization since damping actually varies with the square of velocity. The c_{ij} terms are the static restoring force coefficients. For surge, $c_{11} = 0$ since there is no static restoring force. This is important to note since it means that there is also no resonance problem in surge.

Drag for any body in a fluid consists of pressure or form drag and viscous drag. For bodies on a free surface, there is another form of drag that arises from the generation of surface waves by the body's motion on the surface. This wave drag is of major importance in the study of ship propulsion and is usually determined by Froude scale modeling in a towing tank.

For LULU, no towing tank determination of drag coefficients has been made. An approximate wave drag coefficient can be obtained from Newman '61.

Newman mathematically determined linear wave drag coefficients by calculation of the energy in the generated wave system. His body forms were long ellipsoids located below the free surface. Since LULU'S pontoons break the free surface, the calculated values are low but serve as an estimate for comparison to LULU'S inertial response term. The linear drag coefficient for a submerged ellipsoid of the pontoon's dimensions was $110 \text{ lb}_m - \text{ft./sec.}$

The form drag on the pontoon is given by:
equation 2-17

$$\text{Drag} = \frac{1}{2} \rho S C_D V^2$$

where: S = projected area

ρ = water density

V = velocity

C_D = form drag coefficient.

From Hoerner, the form drag coefficient for a two dimensional shape similar to the pontoon is $C_D = .38$. Again, using 50 square feet as the projected cross-sectional wetted area, the form drag on one pontoon becomes:

$$\text{Drag} = \frac{1}{2} \left(2 \frac{\text{slug}}{\text{ft}^3} \right) (50 \text{ ft}^2) (.38) (V^2) \times 1 \frac{\text{lb}_f - \text{Sec}^2}{\text{sl} - \text{ft}}$$

equation 2-18

$$D_{\text{rag}} = (19 \times V^2) \text{ lb}_f.$$

The inertial response term is the product of LULU'S virtual mass and vehicle acceleration. The added mass coefficient for half of a deeply submerged ellipsoid of the pontoon's dimensions is .015 (Newman '71). Hence, the ratio of LULU'S drag to inertia, β_L , is given by:

$$\beta_L = \frac{bV_L + \frac{1}{2}\rho S C_D V_L^2}{m_L' V_L} = \frac{(110V_L + 19V_L^2) \times 32.2 \frac{\text{lb}_m\text{-ft.}}{\text{lb}_f\text{-sec}^2}}{(1.015)(215 \text{ L.tons})(2240 \frac{\text{lb}_m}{\text{L.ton}})}$$

equation 2-19

$$\beta_L = \frac{110V_L + 19V_L^2}{15200 V_L}$$

If water particle velocity and acceleration are used as an order of magnitude approximation of vehicle velocity and acceleration, equation 2-19 becomes:

$$\beta_L = \frac{110H\omega/2 + 19H^2\omega^2/4}{15200 H\omega^2/2}$$

equation 2-20

$$\beta_L = \frac{17.5T + 9.5H}{1.52 \times 10^4}$$

When using sea state spectra, the best estimator of the average significant wave height is $H^{1/3}$, the average 1/3 highest wave value. The true spectrum average, $H^{1/2}$, is low due to the influence of the small waves which are present in the complete spectrum but are insignificant for engineering applications. For the case at hand, design wave periods of 6, 7 and 8 seconds were used since they covered the sea state 5 to 6 range. The $H^{1/3}$ values were obtained from Marks' data on fully arisen seas in figure 2-3a and Vine and Volkman's sea state chart in figure 2-3b. The $H^{1/3}$ values used were 8.5 feet, 12 feet and 16 feet, respectively. For these conditions, $\beta_L \ll 1$ and the drag term will be neglected.

In the case of ALVIN, model tests have shown that her wave drag is very small for the free surging condition and form and viscous drag predominated. From fully submerged model tests (Mavor '66), ALVIN'S total drag coefficient was $C_D = .027$, based on a wetted area of 500 square feet. This included the presence of the sail which is not effective to drag on the surface. Hence β_A is given by:

$$\beta_A = \left(\frac{1}{2} \rho S C_D V_A^2 \right) / \left(m_A \dot{V}_A \right)$$

Sea State	Wind Vel. (kts)	Wave Height (ft.)			Period (sec)		Length (ft)
		Mean	Sig. $H^{1/3}$	$H^{1/10}$	Max. Energy	Mean	
1	4-7	.18-.6	.29-1	.37-1.2	2-3.4	1.4-2.4	6.7-20
2	7-14	.88-1.8	1.4 -2.9	1.8 -3.7	4-5.4	2.9-3.9	27.0-52
3	14-16	2.0 -2.9	3.3 -4.6	4.2 -5.8	5.6-6.5	4.0-4.6	59.0-71
4	17-20	3.8 -4.3	6.1 -6.9	7.8 -8.7	7.2-7.7	5.1-5.4	90.0-99
5	20-23	5.0 -7.9	9.0 -12	13.0 -16	8.1-9.7	5.7-6.8	111.0-160
6	24-30	8.2 -11	13.0 -18	17.0 -23	9.9-11.3	7.0-7.9	164.0-212

Figure 2-3a. Characteristics of Fully Arisen Sea. (Reproduced from Cohen 1972 - After W. Marks, Geo-Marine Technology Nov. 1964).

WIND WAVES AT SEA
Corresponding values lie on a vertical line.

1 WIND VELOCITY knots	4	5	6	7	8	9	10	20	30	40	50	60	70				
2 BEAUFORT WIND and DESCRIPTION	1 LIGHT AIR	2 LIGHT BREEZE	3 GENTLE BREEZE	4 MODERATE BREEZE	5 FRESH BREEZE	6 STRONG BREEZE	7 MODERATE GALE	8 FRESH GALE	9 STRONG GALE	10 WHOLE GALE	11 STORM						
3 REQUIRED FETCH in MILES	Fetch is the number of miles a given wind has been blowing over open water.							50	100	200	300	400	500	600	700		
4 REQUIRED WIND DURATION in HOURS	Duration is the time a given wind has been blowing over open water.							5	20	25	30	35					
If the fetch and duration are as great as indicated above, the following wave conditions will exist. Wave heights may be up to 10% greater if fetch and duration are greater.																	
5 WAVE HEIGHT CREST to TROUGH in feet																	
6 SEA STATE and DESCRIPTION	1 SMOOTH		2 SLIGHT		3 MODERATE		4 ROUGH		5 VERY ROUGH		6 HIGH		7 VERY HIGH		8 PRECIPITOUS		
7 WAVE PERIOD sec.		1	2	3	4	5	6	8	10	12	14	16	18	20			
8 WAVE LENGTH feet			20	40	60	80	100	150	200	300	400	500	600	800	1000	1400	1800
9 WAVE VELOCITY Knots			5	10	15	20	25	30	35	40	45	50	55	60			
10 PARTICLE VELOCITY feet/sec.		1	2	3	4	5	6	8	10	12	14						
11 WIND VELOCITY knots	4	5	6	7	8	9	10	20	30	40	50	60	70				

Only lines 7, 8, and 9 are applicable to swell as well as to waves.

This table applies only to waves generated by the local wind and does not apply to swell originating elsewhere.

WARNING: Presence of swell makes accurate wave observations exceedingly difficult.

NOTE:

- The height of waves is arbitrarily chosen as the height of the highest 1/3 of the waves. Occasional waves caused by interference between waves or between waves and swell may be considerably larger.
- The above values are only approximate due both to lack of precise data and to the difficulty in expressing it in a single easy way.
- Below the surface the wave motion decreases by 1/2 for every 1/4 of a wave length of depth increase.
- Observations and comments leading to increased accuracy and usefulness are desired.

VINE and VOLKMANN W.H.O.I. JUNE, 1950

Figure 2-3b. Summary of Wind Wave Characteristics (Reproduced from Vine and Volkman 1950).

$$\beta_A = \frac{(\frac{1}{2})(2 \frac{\text{slug}}{\text{ft}^3})(500 \text{ft}^2)(.027) V_A^2 \times 1 \frac{\text{lb}_f\text{-sec}^2}{\text{slug-ft}}}{(1.13)(15 \text{L.tons})(2240 \frac{\text{lb}_m}{\text{L.ton}})(\frac{1}{32.2} \frac{\text{lb}_f\text{-sec}^2}{\text{lb}_m\text{-ft}}) \dot{V}_A}$$

equation 2-21

$$\beta_A = \frac{13.5 V_A^2}{1180 \dot{V}_A}$$

Again, if water particle values for velocity and acceleration are used:

$$\beta_A = \frac{13.5 H^2 \omega^2 / A}{1180 H \omega^2 / 2}$$

So it follows that:

equation 2-22

$$\beta_A = 5.7 \times 10^{-3} H$$

For the previously mentioned sea conditions, $\beta_A \ll 1$.
Again, the drag is neglected.

The resulting response functions for LULU and ALVIN are:

equation 2-23

$$X_A = M_A \dot{V}_A = 1.18 \times 10^3 \dot{V}_A \text{ lb}_f$$

equation 2-24

$$X_L = M_L \dot{V}_L = 1.62 \times 10^4 \dot{V}_L \text{ lb}_f$$

Equating equation 2-23 to equation 2-15 results in:
equation 2-25

$$\dot{V}_A = -2.34 \times 10^4 \left(\frac{H}{T^2} \right) \cos\left(\frac{\pi}{T^2} - \frac{6.28t}{T} \right).$$

Likewise, equating equation 2-24 to equation 2-10
results in:

equation 2-26

$$\dot{V}_L = -.197 H \sin\left(\frac{49}{T^2} \right) \cos\left(-\frac{6.28t}{T} \right).$$

Differentiating equations 2-25 and 2-26 obtains
the following velocity expressions:

equation 2-27

$$V_A = 2.29 \left(\frac{H}{T^2} \right) \sin\left(\frac{\pi}{T^2} - \frac{6.28t}{T} \right).$$

equation 2-28

$$V_L = .0312 (H \times T) \sin\left(\frac{49}{T^2} \right) \sin\left(-\frac{6.28t}{T} \right).$$

All assumptions made here were conservative,
that is, they tended to increase the surge velocities
and the response-phase difference of the vehicles.
Hence, the collision energy was maximized.

Energy Analysis

Figure 2-4 shows the sequence of collisions

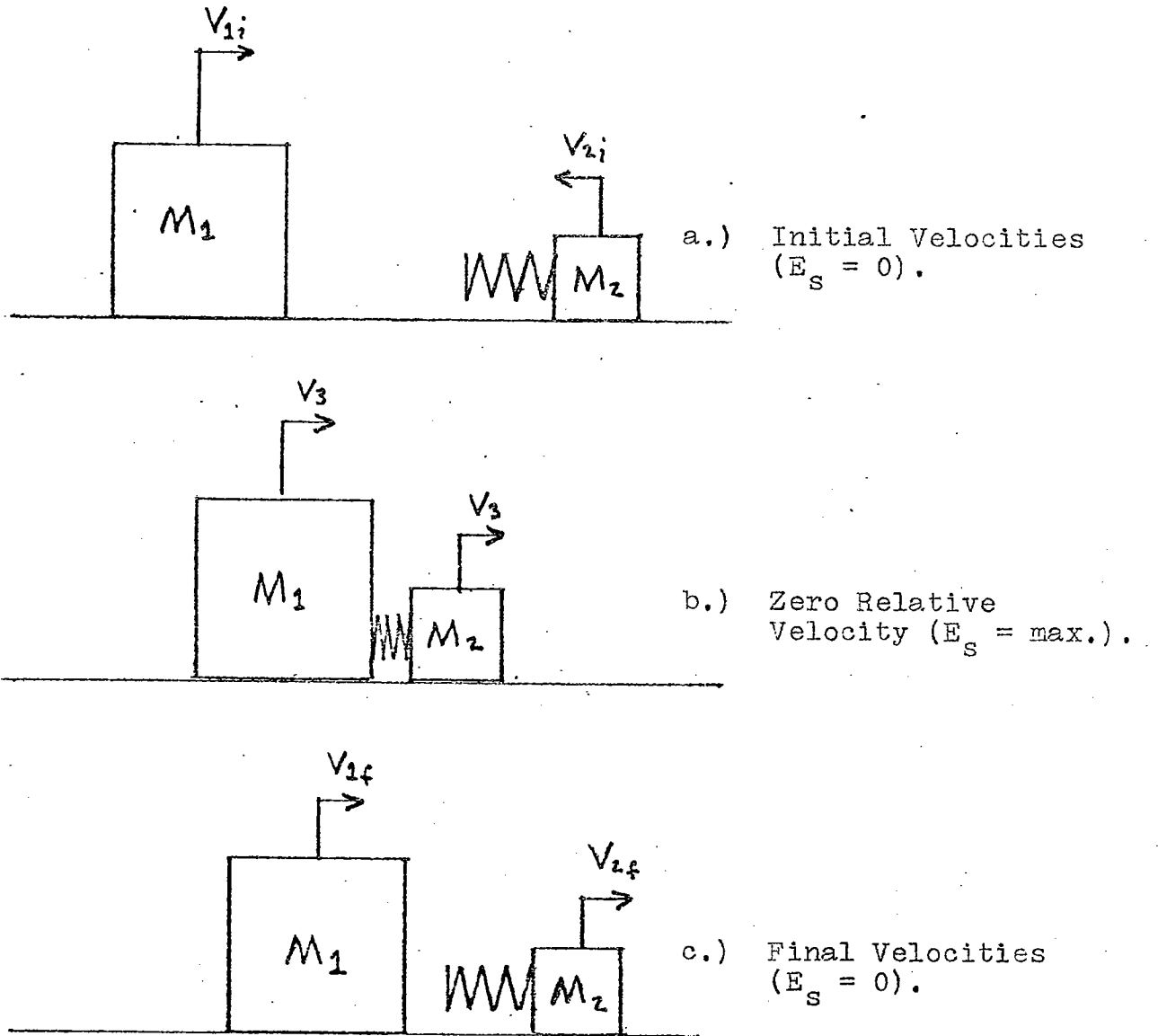


Figure 2-4. Collision of Two Masses.

between two masses with a linear elastic spring attached to one of the masses. Energy and momentum are conserved in the collision so that the expressions for total energy and momentum are constant for the three states shown. In figure 2-4a, the two masses approach each other with initial velocities. In figure 2-4b, the two masses move with the same velocity. At this point the relative velocity between the two bodies is zero and the energy absorbed by the spring is at a maximum. In figure 2-4c, both bodies are moving at their final velocities and there is no energy retained in the spring. The equations for conservation of energy and momentum are:

equation 2-29

$$\frac{1}{2} V_1^2 M_1 + \frac{1}{2} V_2^2 M_2 + E_s = E_T = \text{constant}$$

equation 2-30

$$M_1 V_1 + M_2 V_2 = \text{Mom}_T = \text{constant}$$

where: E_s = spring energy

E_T = total energy

Mom_T = total momentum.

For figure 2-4a, the calculated values of surge velocity for LULU and ALVIN are used:

equation 2-31

$$\frac{1}{2} V_L^2 M_L' + \frac{1}{2} V_A^2 M_A' + 0 = E_T$$

equation 2-32

$$M_L' V_L + M_A' V_A = M_{omT}$$

Note that M_L' will be the total virtual mass of LULU with both pontoons. Likewise, M_A' will be the virtual mass of ALVIN.

For figure 2-4b:

equation 2-33

$$\frac{1}{2} V_3^2 (M_L' + M_A') + E_S = E_T$$

equation 2-34

$$V_3 (M_L' + M_A') = M_{omT}$$

If equation 2-32 is equated to equation 2-34, V_3 becomes:

equation 2-35

$$V_3 = \frac{M_L' V_L + M_A' V_A}{M_L' + M_A'}$$

Now E_s can be determined by equating equation 2-31 to equation 2-33:

equation 2-36

$$E_s = \frac{1}{2} M_L' (V_L^2 - V_3^2) + \frac{1}{2} M_A' (V_A^2 - V_3^2).$$

Using previously given values for virtual mass, equations 2-35 and 2-36 become:

equation 2-37

$$V_3 = \left[\frac{9.8 \times 10^5 V_L + 3.8 \times 10^4 V_A}{1.018 \times 10^6} \right] \frac{\text{ft.}}{\text{sec.}}$$

equation 2-38

$$E_s = \left[1.525 \times 10^4 (V_L^2 - V_3^2) + 5.9 \times 10^2 (V_A^2 - V_3^2) \right] \text{ft.-lb}_f.$$

Bumper Geometric Analysis

The two main ballast spheres on ALVIN are 11.5 inches in radius and pressurized with air to 2500 psi. The initial volume then is:

equation 2-39

$$V_i = 2 \left(\frac{4}{3} \pi R^3 \right) = 1.28 \times 10^4 \text{in}^3$$

Since bumper inflation and collision compression are both rapid processes, isentropic conditions will be assumed. The isentropic gas relation is:

equation 2-40

$$P_i V_i^\gamma = \text{constant}$$

where $\gamma = c_p/c_v = 1.4$ for air.

Final bumper volume is given by the product of the cross-sectional area and mean bumper perimeter. The cross-section will be elliptical and the mean perimeter will be the equivalent straight length of the bumper. Hence, final volume is:

equation 2-41

$$V_f = (\pi a_o b_o) L_m + V_i$$

where: a_o = minor radius

b_o = major radius

L_m = mean perimeter (refer to figure 2-5).

Again, if the isentropic gas relation is used, final bumper pressure is:

equation 2-42

$$P_f = P_i \left(\frac{V_i}{V_f} \right)^\gamma$$

Once the bumper has been inflated, valves connecting the air tanks and the bumper will be

closed. Hence, the system's new initial volume will be:

equation 2-43

$$V_1 = V_f - V_i = (\pi a_o b_o) L_m$$

equation 2-44

$$P_1 = P_f$$

The expression for work done on compressing a gas is:

equation 2-45

$$W = \int_{V_1}^{V_2} P dV$$

If the isentropic gas law is used, equation 2-45 becomes:

equation 2-46

$$W = P_1 V_1^{\gamma} \int_{V_1}^{V_2} \frac{dV}{V^{\gamma}} = P_1 V_1^{\gamma} \left[\frac{V^{(1-\gamma)}}{1-\gamma} \right]_{V_1}^{V_2}$$

Solving for V_2 :

equation 2-47

$$V_2 = \left[\frac{W(\gamma-1)}{P_1 V_1^{\gamma}} + V_1^{1-\gamma} \right]^{\frac{1}{1-\gamma}}$$

Therefore, the necessary change in volume to absorb the energy of collision, E_s , is given by:

equation 2-48

$$\Delta V = V_1 - \left[E_s (\gamma - 1) / (\rho_1 V_1^{\gamma-1}) + V_1^{\frac{1-\gamma}{1-\gamma}} \right]$$

where the terms on the right hand side are known from the specification of the bumper geometry and from the energy of collision analysis.

Figure 2-5 shows water line 4 with bumper inflated. Collision with LULU is simulated by a straight line of contact compressing the bumper by a penetration depth, d . The semi-circular bow is selected as the collision location because this is the bumper region with the smallest radius of curvature. The smaller the radius of curvature, the larger the penetration depth, d , will be. The undisturbed bumper width is $2a_0$. In the compressed regions, the width is $2a(\phi)$ where $\phi = \theta - \theta_0$. The differential equation for volume anywhere in the bumper is:

equation 2-49

$$dV = (R+a) \pi a b d\phi$$

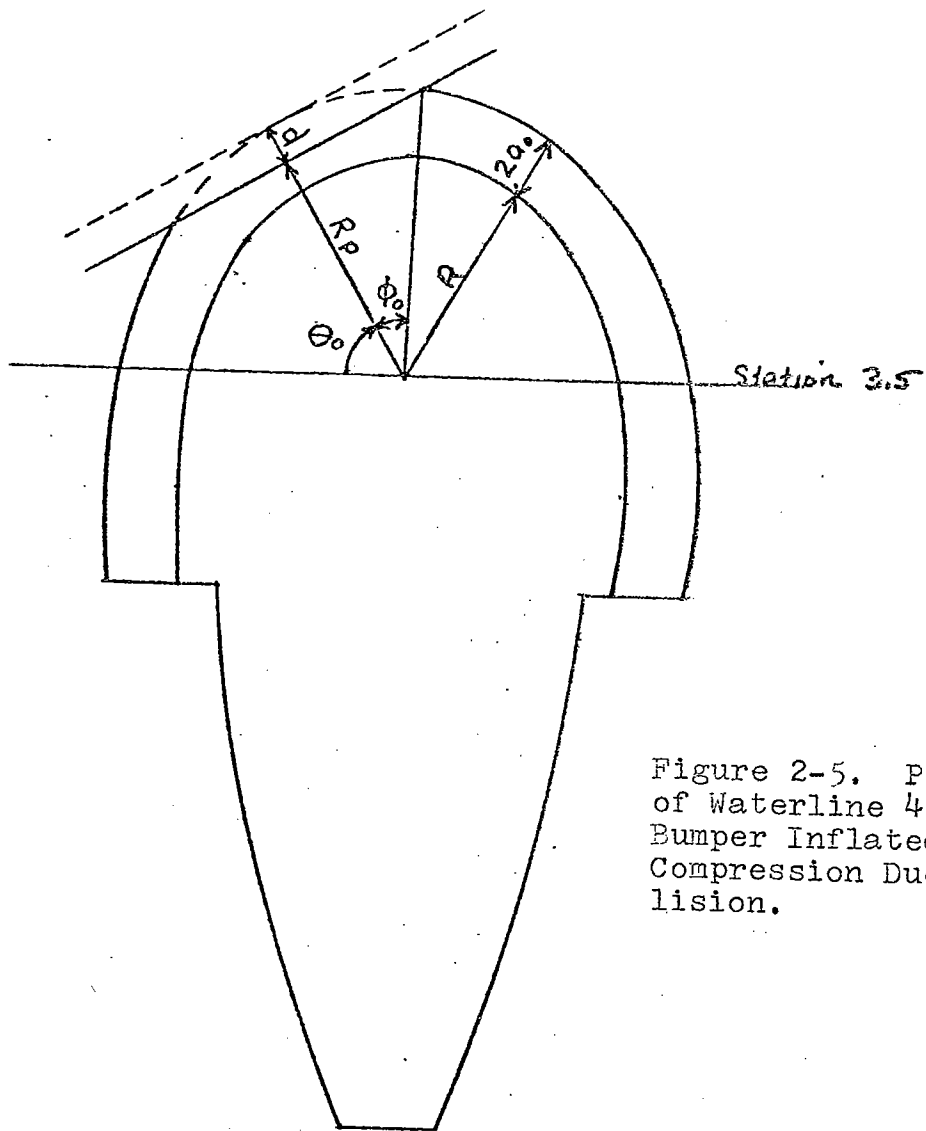
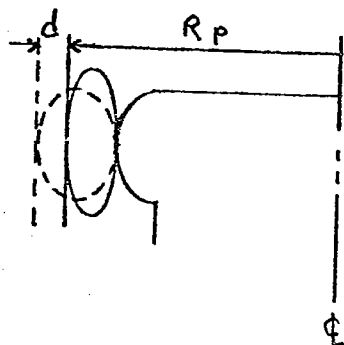


Figure 2-5. Plan View of Waterline 4 with Bumper Inflated Showing Compression Due To Collision.

Sec. at $\theta = \theta_0$



5 4 3 2 1 0
Scale 1/4":1'

where: R = uninflated radius

b = $\frac{1}{2}$ bumper depth

A constant section perimeter restraint will be imposed which is valid considering that the bumper's neoprene skin will stretch very little due to its dacron chord backing. With this: equation 2-50 bumper perimeter $\approx 2\pi \left[\frac{a_0^2 + b_0^2}{2} \right]^{\frac{1}{2}} = \text{constant}$.

Solving for b in the compressed region results in:

equation 2-51

$$b = \left[a_0^2 + b_0^2 - a^2 \right]^{\frac{1}{2}}$$

The differential volume equation becomes:

equation 2-52

$$dV = \pi a \left[a_0^2 + b_0^2 - a^2 \right]^{\frac{1}{2}} (R + a) d\phi$$

Again, considering figure 2-5, the following trigometric relation is obtained:

equation 2-53

$$\cos \phi = \frac{R_2 - d}{R + 2a} = \frac{R_p}{R + 2a}$$

where: R_p = the protected radius = $R_2 - d$

Solving for $a(\phi)$:

$$a(\phi) = \frac{1}{2} \left[\frac{R_p}{\cos(\phi)} - R \right]$$

equation 2-54

$$a(\phi) = \frac{1}{2} \left[R_p \sec(\phi) - R \right]$$

Now the total angle ϕ_0 of the compressed region of the bumper is:

$$\cos(\phi_0) = \frac{R_p}{R + 2a_0}$$

equation 2-55

$$\phi_0 = \cos^{-1} \left(\frac{R_p}{R + 2a_0} \right)$$

The volume of the compressed region of the bumper is obtained by numerically integrating equation 2-52. A sixth order Simpson Rule formula was used by dividing the total angle of the affected region, $2\phi_0$, by 6. For each $\Delta\phi$ increment, $a(\phi)$ was obtained from equation 2-54 and substituted into equation 2-52. The resulting volume was subtracted from the original volume of the section, $2\phi_0 \pi a_0 b_0 (R + a_0)$, and the ΔV as function of a_0 for various R_p 's was obtained.

The protected regions on ALVIN can now be determined as a function of various geometric parameters of the bumper. These parameters are:

- (1) bumper depth, b_0
- (2) bumper width, a_0
- (3) uninflated radius, R
- (4) total bumper length, specified by the stations number to which the bumper extends.

CHAPTER 3

RESULTS

Surge Velocities and Energy of Collision

Figures 3-1, 3-2, and 3-3 show the surge velocities of LULU and ALVIN and the resulting collision energies. The collision energy curve does not extend below $E_s = 0$ since this is the region of non-collision between LULU and ALVIN.

The crest of the energy curve increases and shifts to the left with increasing wave periods and wave heights. The shift to the left can be seen by looking at the energy curve crest in relation to the half period point. In figure 3-1, the crest is to the right of 3 seconds. In figure 3-2, the crest occurs very near 3.5 seconds. In figure 3-3, the crest occurs to the left of 4 seconds.

The explanation of the energy curve's variation is:

- (1) With increasing periods, the phase difference of the two vehicles decreases. This would tend to decrease the collision energy with increasing sea state except for the following fact.

- (2) With increasing wave height the magnitude of the surge velocities increases. Hence, increasing the wave period and wave height produces counteracting effects with the increasing wave height predominating.

The collision energy crest value in figure 3-3, approximately 10,000 ft.-lb_f., will be used in the bumper design analysis.

Geometric Analysis of Bumper

As mentioned at the end of the analysis section, the ΔV necessary to absorb the collision energy and the ΔV available for various protection radii, R_p , are functions of bumper geometry. Figure 3-4 shows the results for a bumper depth of 2 feet ($b = 1$ foot), an uninflated radius $R = (3.5 + a_0)$ feet (where 3.5 feet is the waterline $\frac{1}{4}$ radius at the bow), and a protection perimeter extending to station 8. The points of intersection between the energy curve (which goes from zero to the upper right) and the protection radius curves give the bumper half widths necessary for the various protection radii. To give an idea of the extent of the protection perimeter, an R_p of 5.5 feet is necessary to protect the mechanical arm in the folded position.

Figure 3-5 shows the displacement of the bumper described in figure 3-4. It can be seen that if the present main buoyancy of 1500 lb_f. is retained, the resulting protection radius is less than that which is necessary to protect the mechanical arm.

The buoyancy of the bumper can be decreased by shortening the length of the bumper and/or by decreasing the bumper depth. Figure 3-6 shows the displacement for a bumper with depths of 2 feet and 1.5 feet ($b = 1.0$ and $.75$ feet), uninflated radius $R = (3.5 + a_0)$ feet., and a protection perimeter only extending to station 3.5.

Figure 3-7 shows the protection radius curves for this set of conditions. It can be seen that for the same displacement, the $b = .75$ bumper affords the greater protection radius. Still the protection radius is less than that necessary to protect the mechanical arm.

The protection radius can be extended by increasing the uninflated radius, R . Figures 3-8 and 3-9 show the result. In figure 3-8, the uninflated radius is increased to $R = (4.0 + a_0)$ feet, while the other parameters remain constant. In figure 3-9, the uninflated radius is extended $\frac{1}{2}$ foot more

to $R = (4.5 + a_0)$ feet. The energy curve increases slightly with increasing uninflated radius while the protection radius curves shift $\frac{1}{2}$ foot to the left.

Figure 3-10 shows the buoyancy curves for these two cases. Again, if present main buoyancy of 1500 lb_f is maintained, it can be seen that the protection perimeter extension is very near equal to the increase in uninflated radius.

Figure 3-11 shows the major shortcoming of any inflatable bow bumper. This is the graph of the trim moment created about the center of gravity when the bumper is inflated. The two cases shown are for the bumper geometries used in figures 3-9 and 3-10

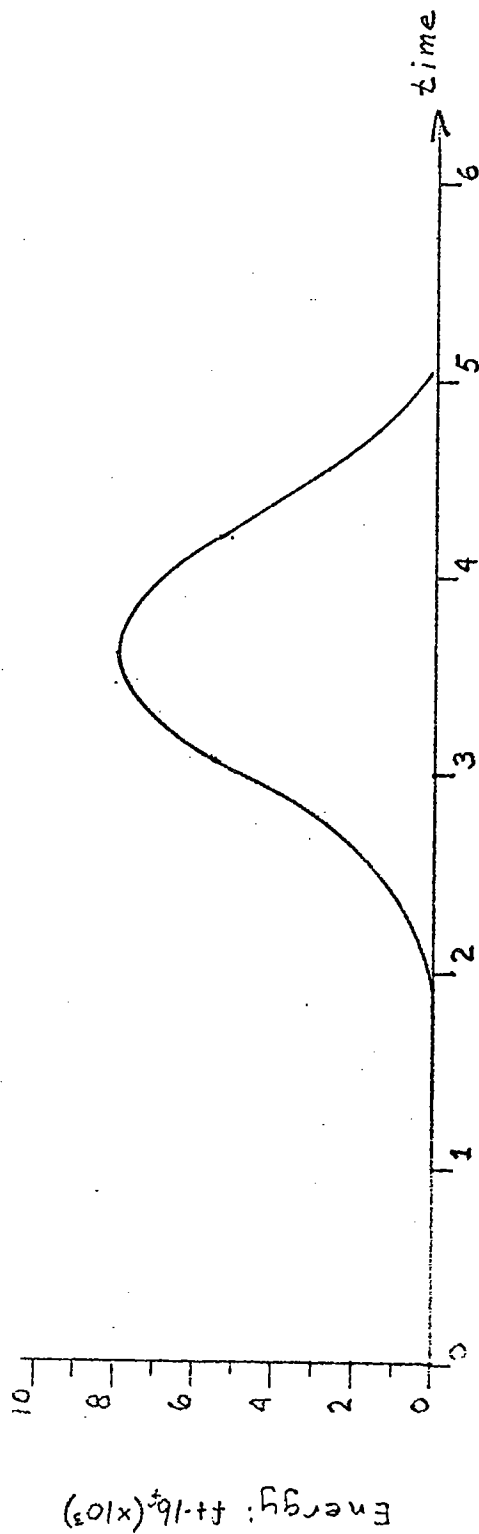
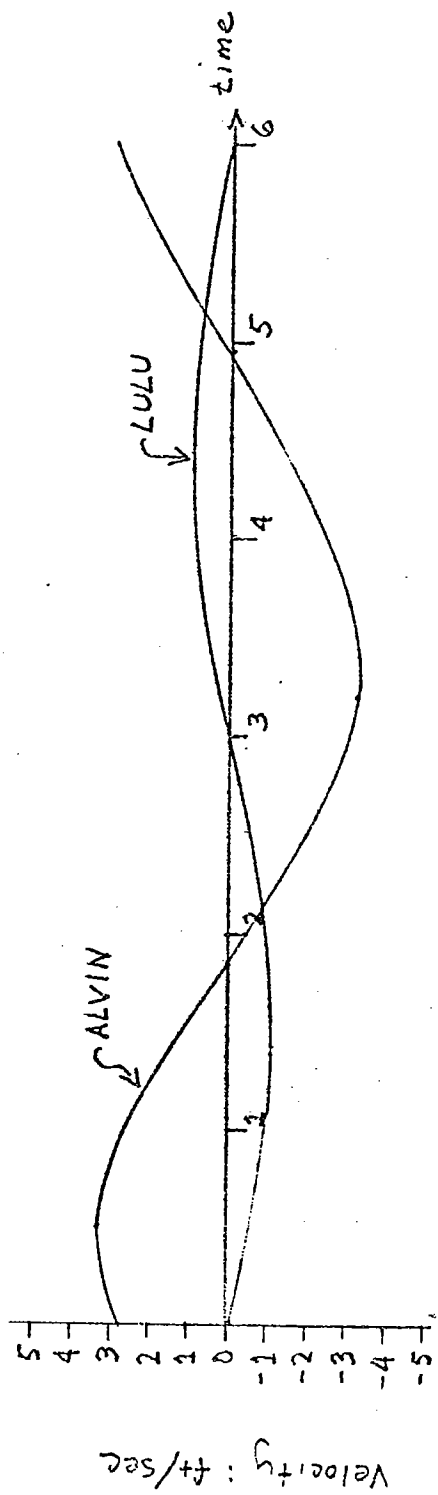


Figure 3-1. Surge Velocity and Collision Energy (T = 6 sec., H = 8.5 ft.).

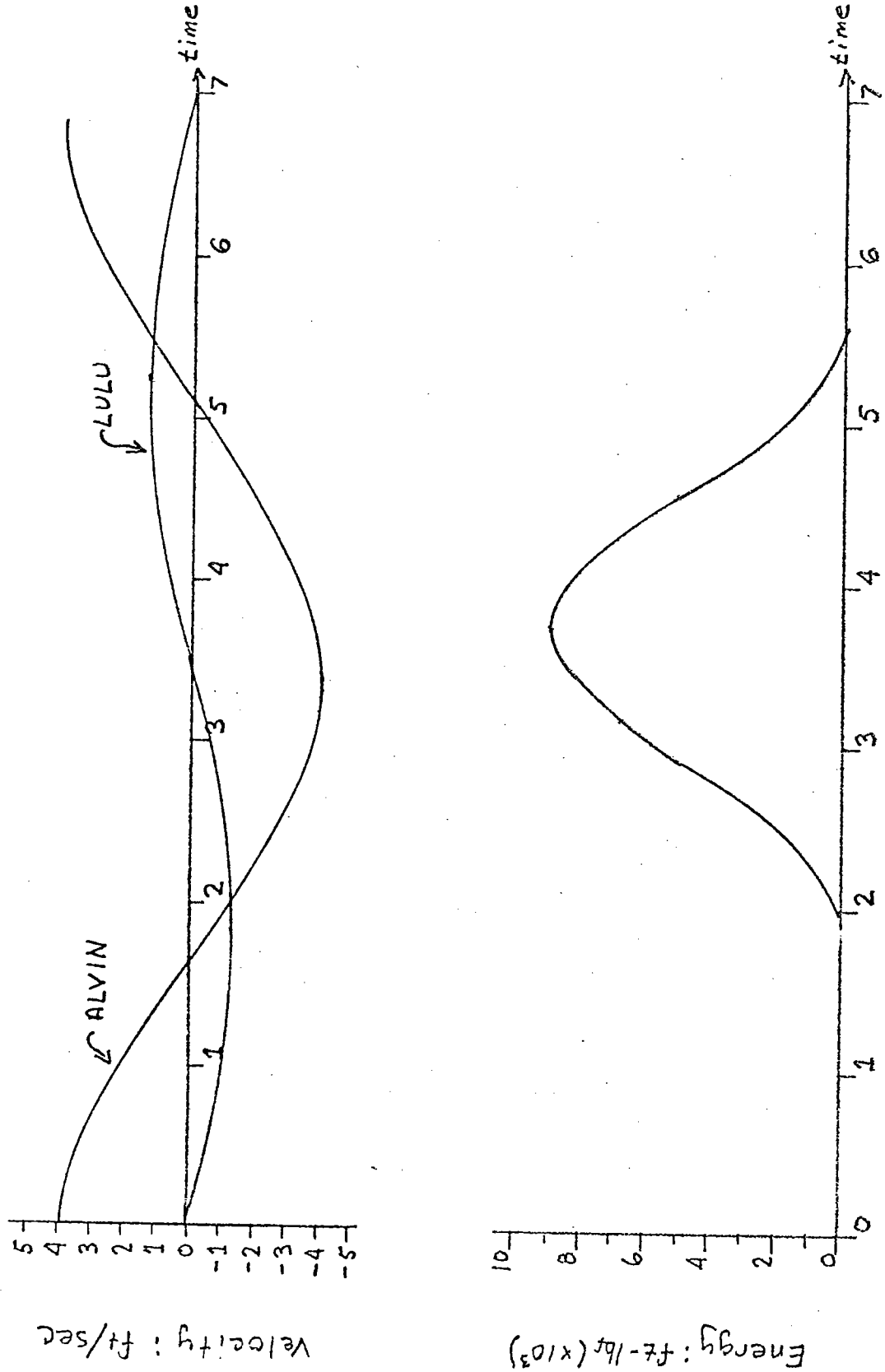


Figure 3-2. Surge Velocity and Collision Energy (T = 7 sec., H = 12 ft.).

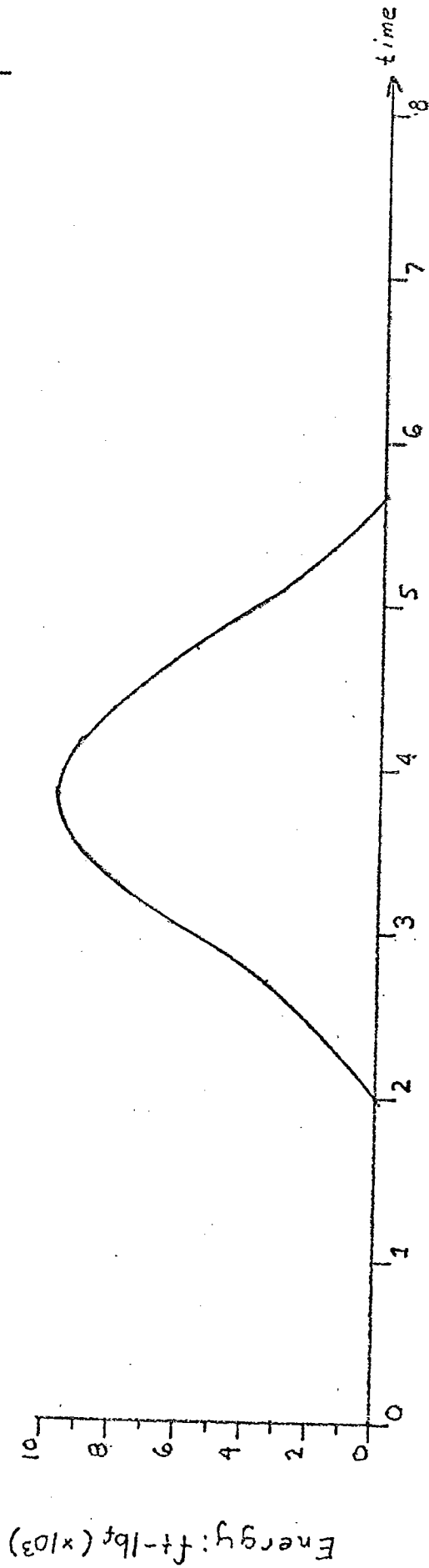
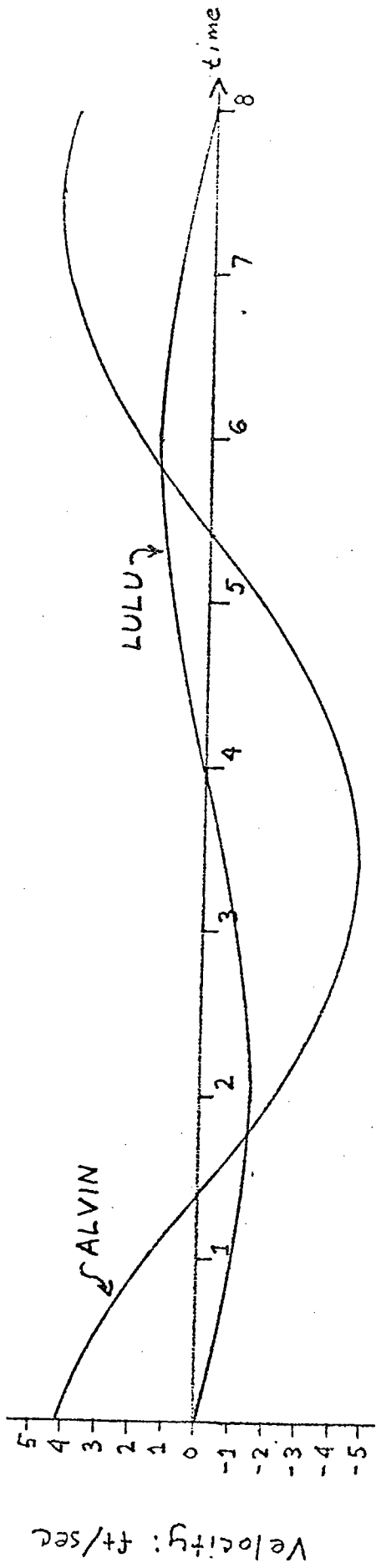


Figure 3-3. Surge Velocity and Collision Energy ($T = 8$ sec., $H = 16$ ft.).

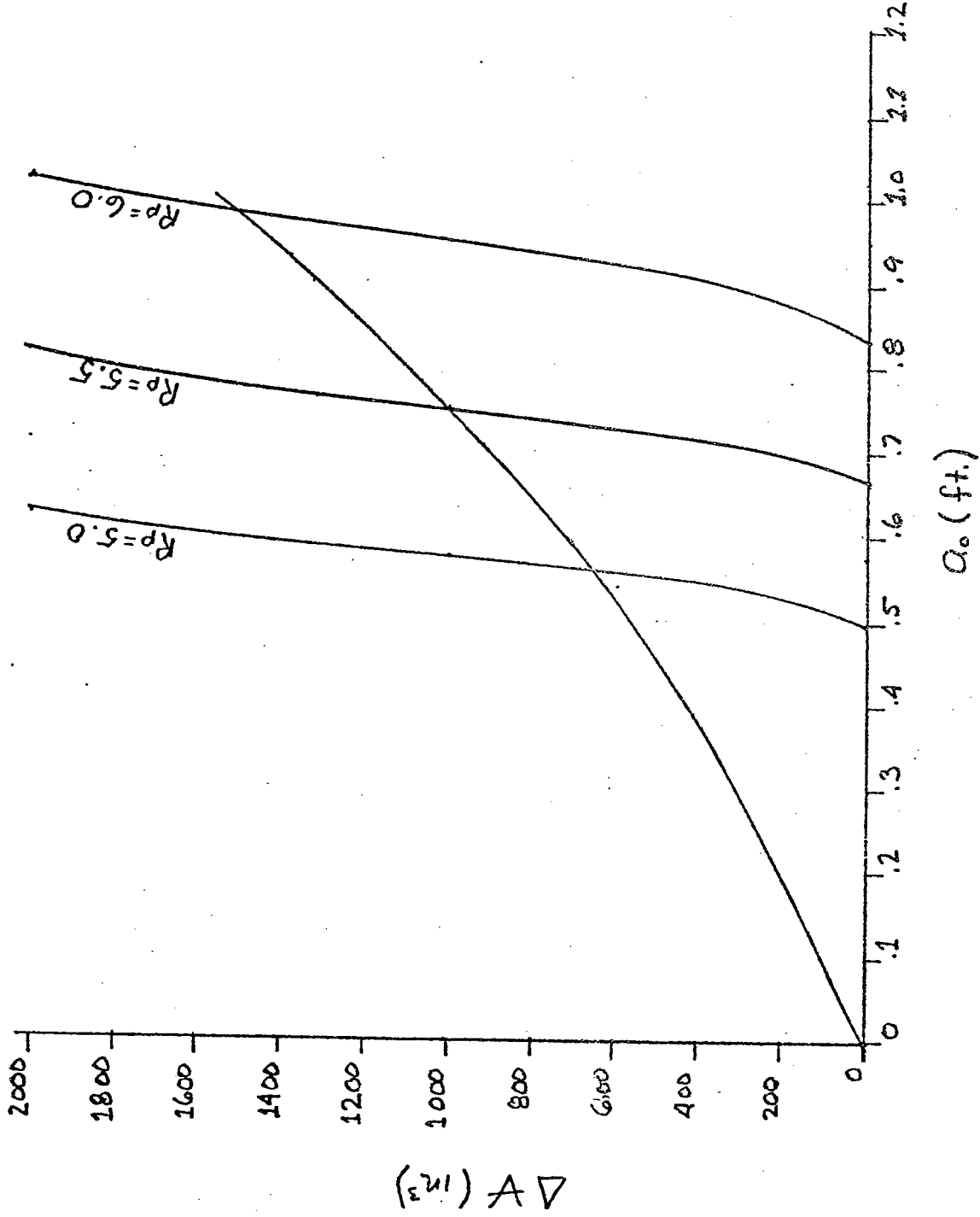


Figure 3-4. Protection Radius Curves ($b_0 = 1.0$ ft., $R = 3.5$ ft., $+ a_0$, to station 3).

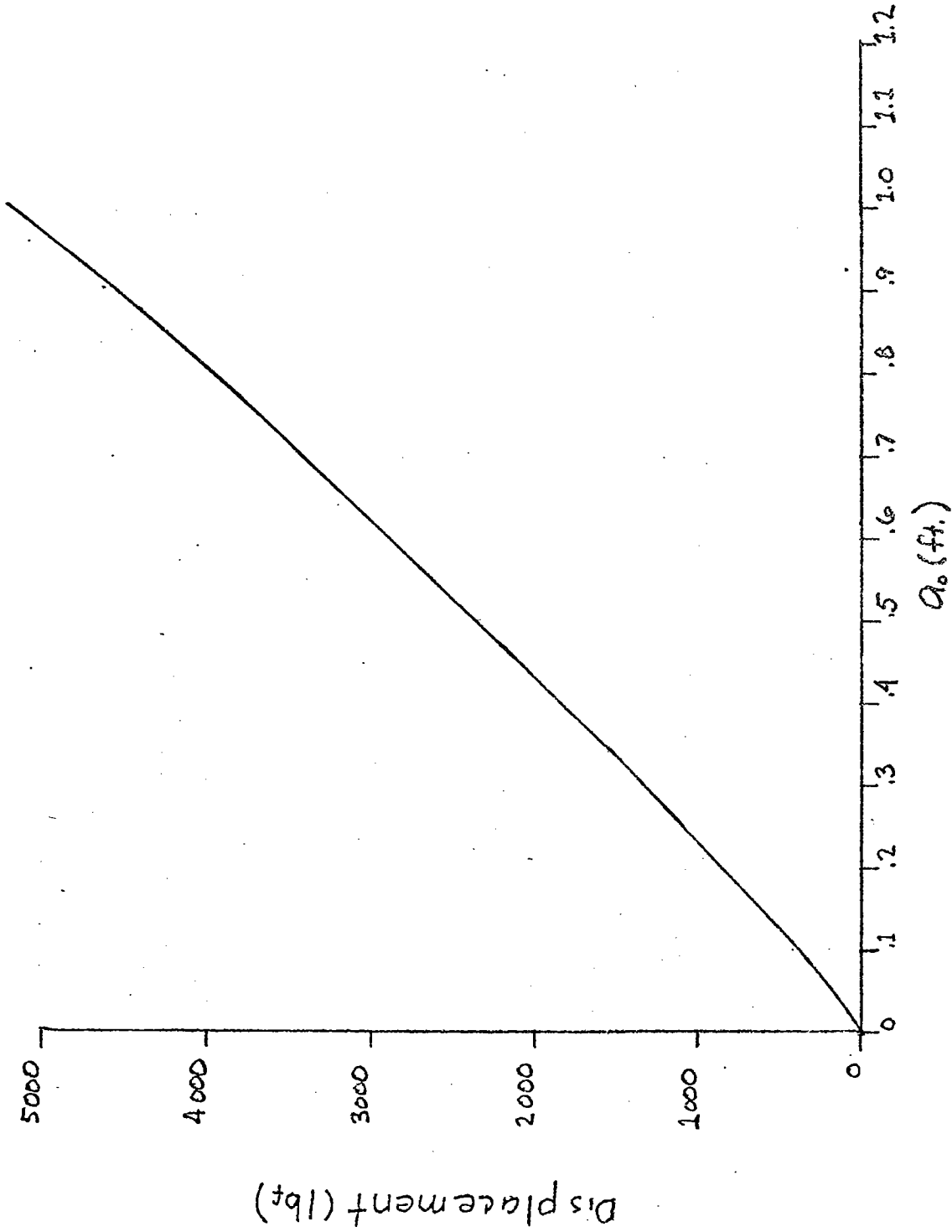


Figure 3-5. Bumper Displacement ($b_0 = 1.0$ ft., $R = 3.5$ ft. + a_0 , to station 8).

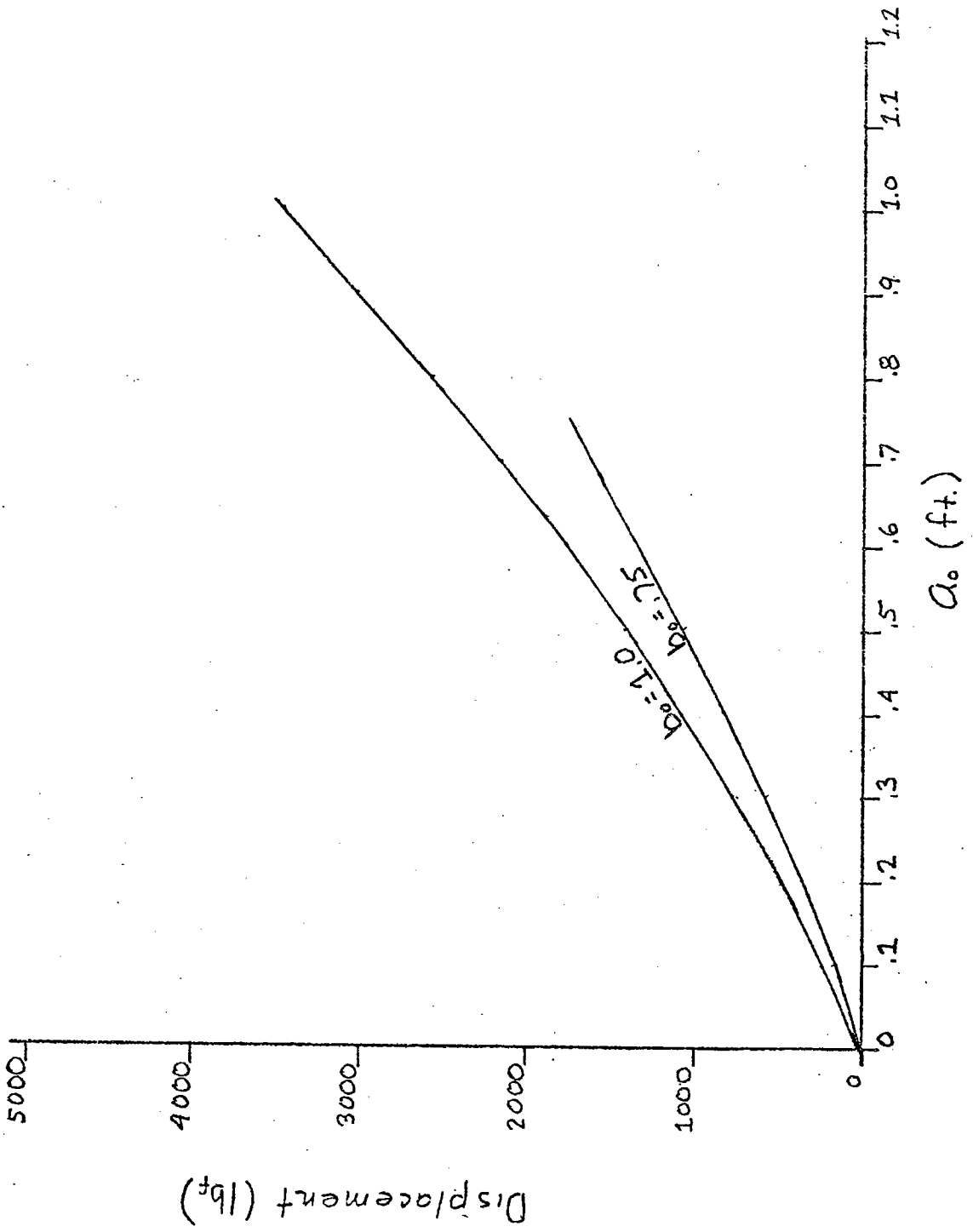


Figure 3-6. Bumper Displacement ($b_0 = .75$ ft. & 1.0 ft., $R = 3.5$ ft. + a_0 , to station 3.5).

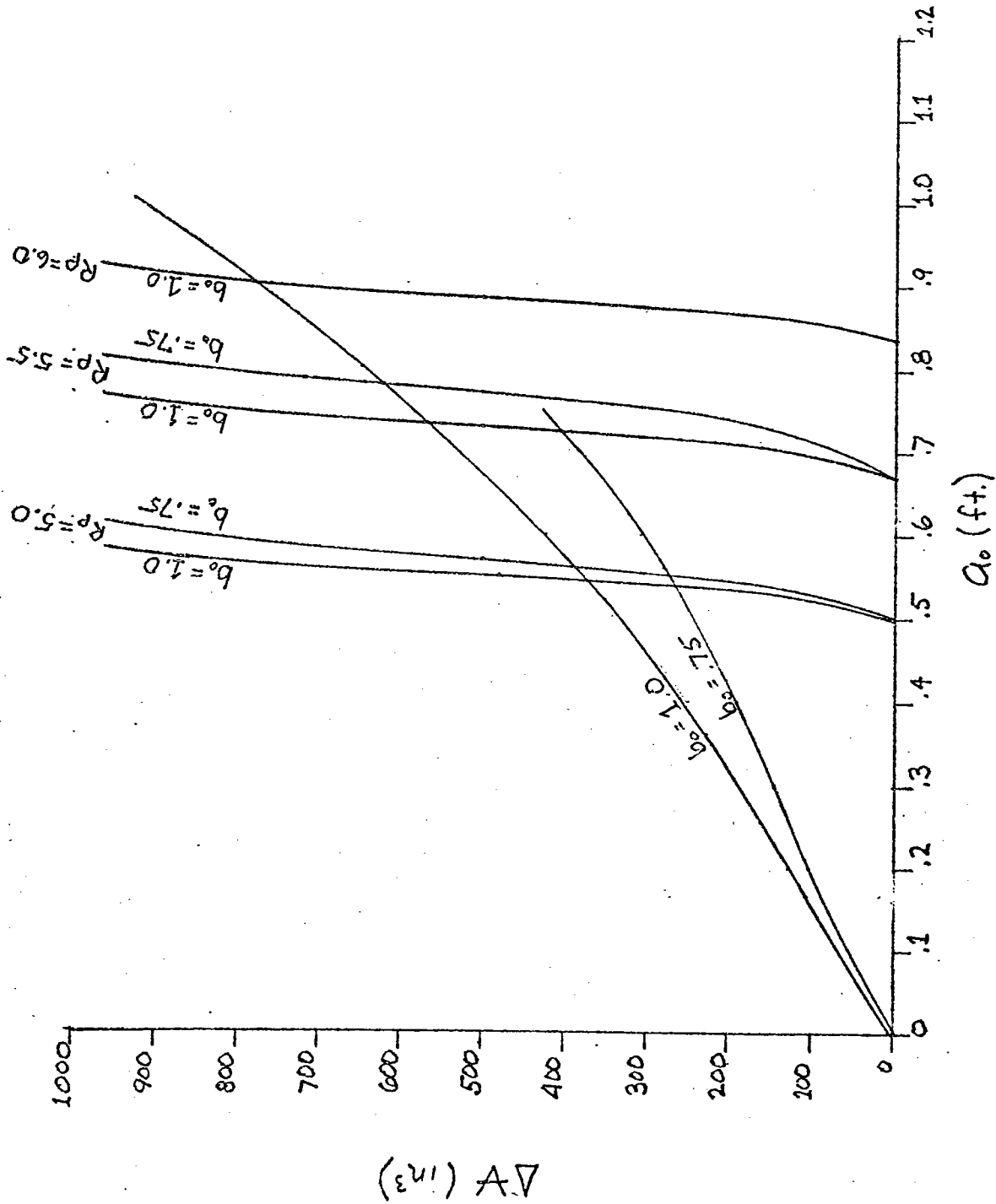


Figure 3-7. Protection Radius Curves ($b_0 = .75$ & 1.0 ft., $R = 3.5$ ft. + a_0 , to station 3.5).

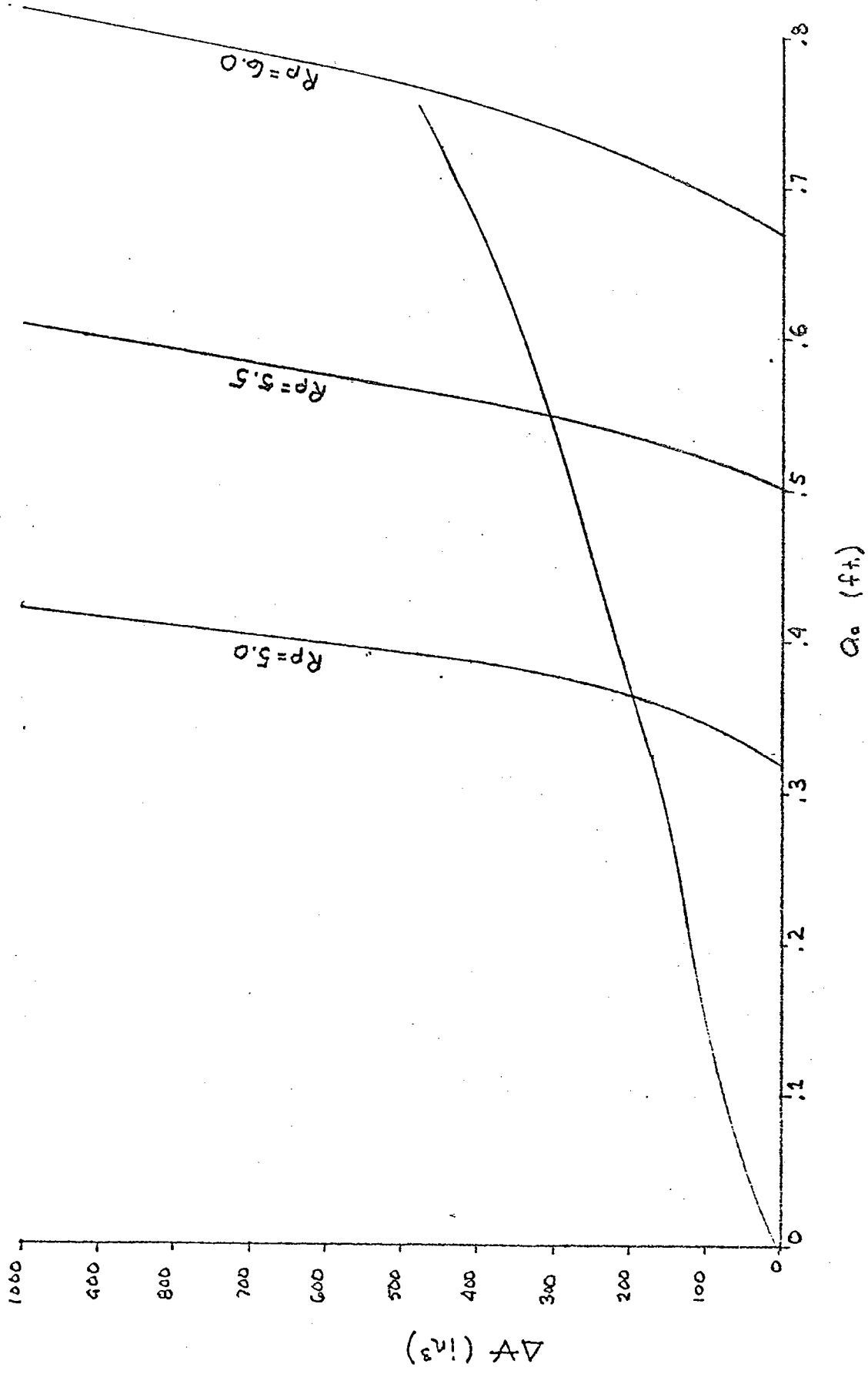


Figure 3-8. Protection Radius Curves ($b_0 = .75$, $R = 4.0$ ft. + a_0 , to station 3.5).

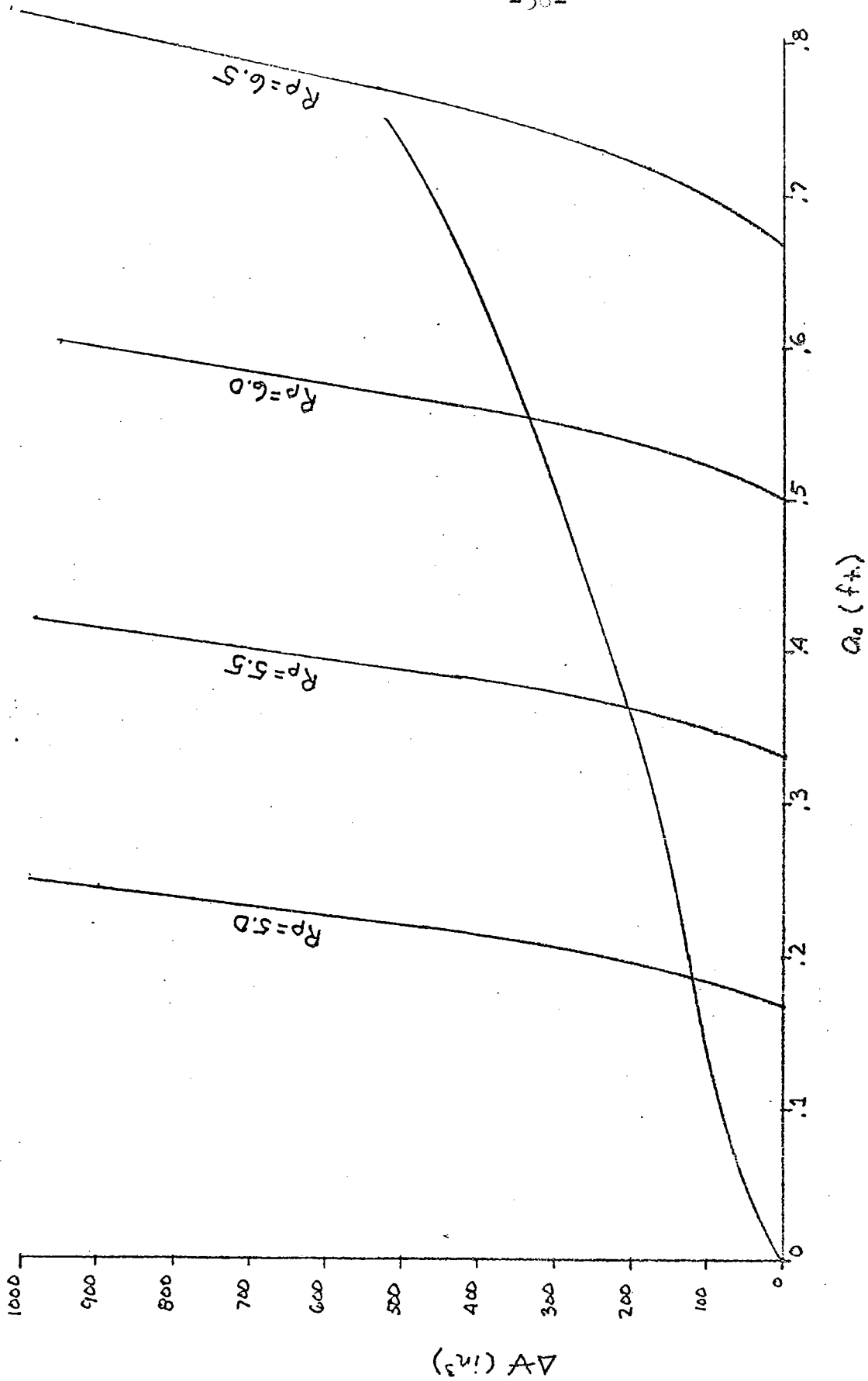


Figure 3-9. Protection Radius Curves ($b_0 = .75$ ft., $R = 4.5$ ft. + a_0 , to station 3.5).

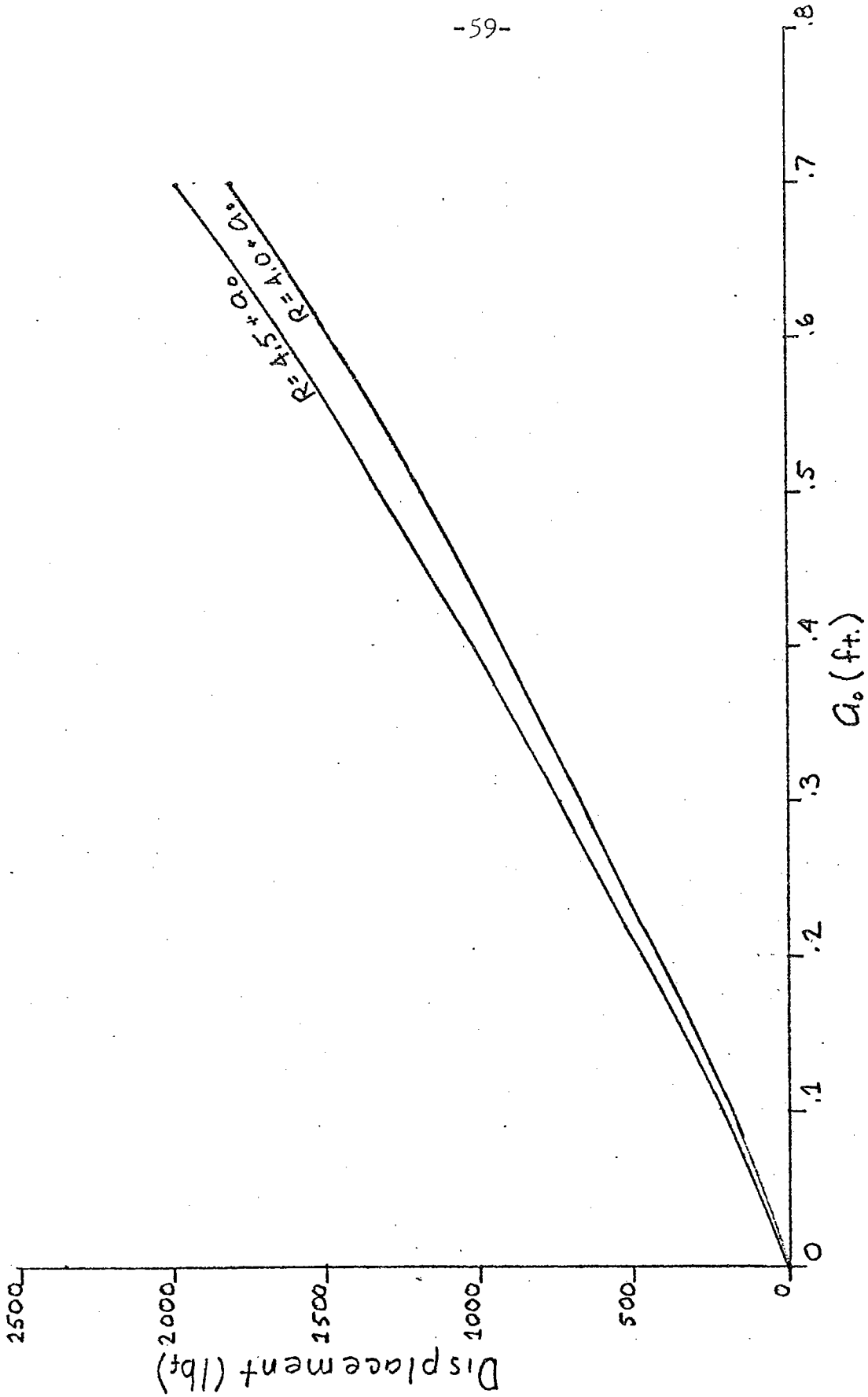


Figure 3-10. Bumper Displacement ($b_0 = .75$ ft., $R = 4.0$ ft., $R = 4.5$ ft., $+ a_0$ & 4.5 ft., $+ a_0$, to station 3.5).

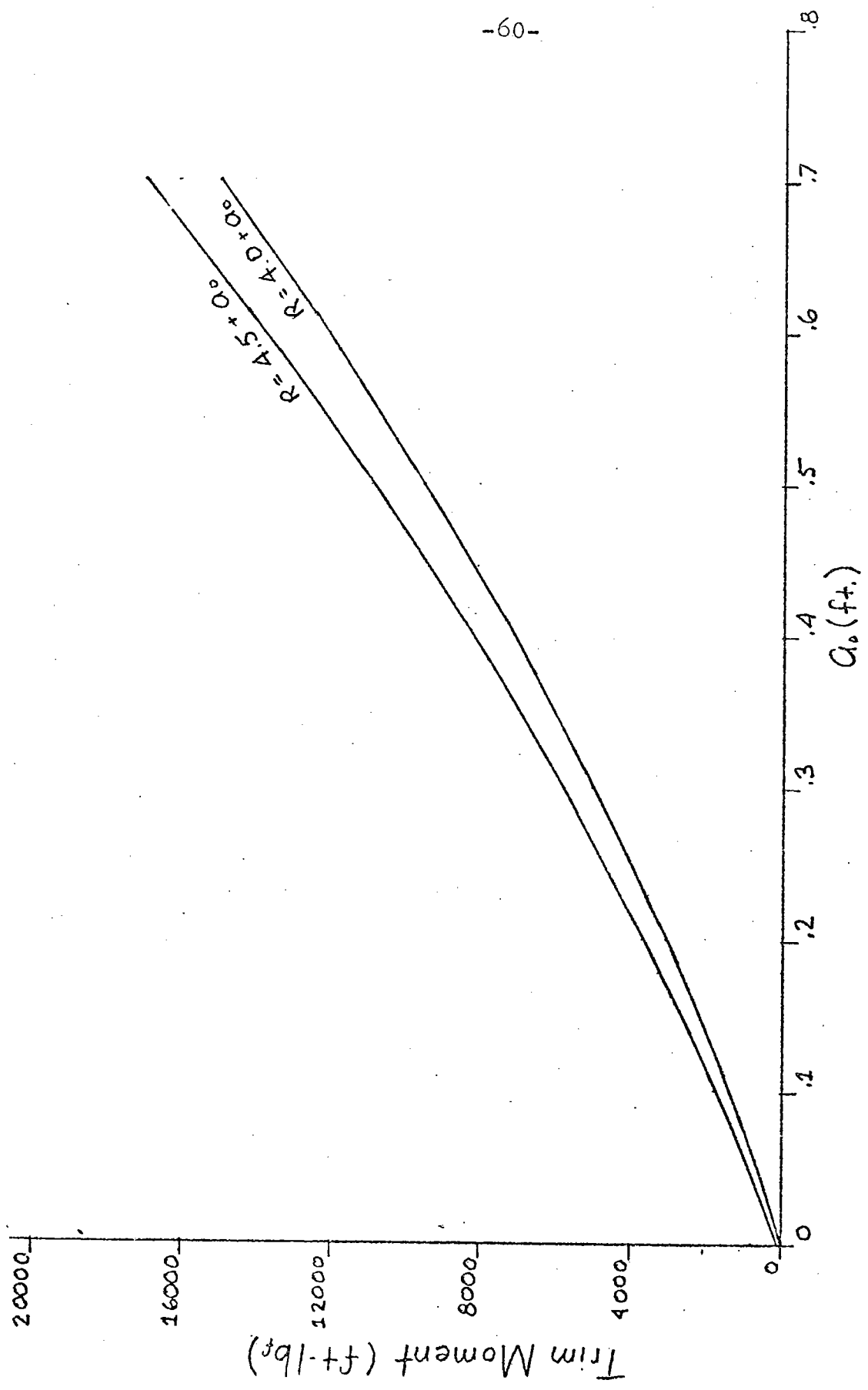


Figure 3-11. Trim Moment About C. G. ($b_0 = .75$ ft., $R = 4.0$ ft., $+ a_0$ & 4.5 ft. $+ a_0$, to station 3.5).

CHAPTER 4

DISCUSSION

(1) A limit to increasing the uninflated radius for the purpose of extending the protection perimeter about the bow is the increasing vertical drag. The drag increases with the increasing projected vertical area. This decreases the terminal ascent and descent velocity of ALVIN, which obviously increases the ascent and descent time.

To give an idea of the approximate time change involved, the bumper geometries in figures 3-9 and 3-10, which yield a displacement of 1500 lb_f, are compared. The resulting difference in the total vertical, projected area is approximately 5%. The equation for terminal velocity is:

equation 4-1

$$V = \left[2W_{\text{wet}} / \rho S C_D \right]^{1/2}$$

where C_D = drag coefficient

W_{wet} = wet weight

S = projected vertical area

ρ = water density

It follows by dimensional analysis that the ratio of terminal velocities for two bodies with different projected areas but equal drag coefficients and wet weight is:

equation 4-2

$$V_1/V_2 = \left[S_2/S_1 \right]^{1/2} .$$

The travel time for a given depth is inversely proportional to the velocity. Therefore, the percent of time increase, $\Delta t\%$, is given by:

$$\Delta t \% = \left(1 - \frac{t_2}{t_1} \right) \times 100\%$$

equation 4-3

$$\Delta t \% = \left[1 - \sqrt{S_2/S_1} \right] \times 100\%$$

For the previously stated case of an area increase of 5%, the resulting $\Delta t\%$ is approximately 2.5%. For a travel time of 2 hours, this means an increase of approximately 3 minutes. Therefore, the protection perimeter can be extended modestly without

greatly increasing descent or ascent time.

(2) The bumper, as described, is a non-linear spring whose expression for Hooke's Law would be of the polynomial form:

equation 4-4

$$F_{\text{spring}} = K_0 + K_1 x + K_2 x^2 + K_3 x^3 + \dots$$

The coefficients in this polynomial would have to be determined numerically.

The expression for energy within the spring is given by:

equation 4-5

$$E_s = \int_0^d F_{\text{spring}} dx .$$

The energy analysis in CHAPTER 2 gives the value of energy for the limits of equation 4-5 (at 0 and penetration depth, d). Since $E_s = 0$ at $x = 0$, it follows that $K_0 = 0$. If the bumper is modeled as linear, then K_1 is determined from equation 4-5 and the rest of the K's are set equal to zero.

This approximation gives a low value of maximum

spring force. A more conservative approximation would be to assume a second order expression for Hooke's Law:
equation 4-6

$$F_{\text{spring}} \approx K_2 x^2$$

With equation 4-6, equation 4-5 can be integrated to yield the following expression for K_2 :
equation 4-7

$$K_2 = \frac{3E_s}{d^3}$$

Hence, the expression for maximum spring force becomes:
equation 4-8

$$F_{\text{spring}} \approx \frac{3E_s}{d}$$

Note that the value of the number on the right hand side of equation 4-8 will increase by 1 for every increase in the assumed order of Hooke's Law.

The maximum deceleration of ALVIN can now be

determined from the equation of motion:
equation 4-9

$$\dot{V}_A = \frac{3Es}{m_R d}$$

The above equation neglects the influence of the waves on ALVIN during collision.

The penetration depth can be expressed as a function of the bumper geometry:
equation 4-10

$$d = R + 2a_0 - R_p$$

where: R = uninflated radius

a_0 = $\frac{1}{2}$ bumper width

R_p = protection radius.

Choosing the geometry of figure 3-9 for a displacement of 1500 lb_f (figure 3-10), the $\frac{1}{2}$ bumper width ($a_0 \approx .55$) and the protection radius $R_p = 6$ feet, the maximum collision force and deceleration is then:

$$F_{\text{collision}} = \frac{(3)(1000 \text{ ft} \cdot \text{lb}_f)}{(4.5 + .55 + 1.1 - 6) \text{ ft}} = 4.0 \times 10^5 \text{ lb}_f$$

$$\dot{V}_A = \frac{4.0 \times 10^5 \text{ lb}_f \times g \frac{\text{lb}_m\text{-ft}}{\text{lb}_f\text{-sec}^2}}{152. \text{ tons} \times 2240 \frac{\text{lb}_m}{\text{L. ton}}}$$

$$\dot{V}_A = 11.6 g$$

The force involved in the above collision is too large for the present structural configuration of ALVIN. The force could be lowered by softening the interior of the pontoons (i.e. water bumper or foam). Also, the number of mechanical links between the fore and afterbodies of ALVIN could be increased beyond the single latch at the base of the personnel sphere. These latches could be triggered by the pilot once the submersible has reached the surface, and inflated the bumper.

Even with these schemes, the forces involved would be great. From equation 4-8, it is seen that the collision force could be reduced by softening the bumper and allowing a larger penetration depth. Disregarding, for the moment, the bumper geometry and surface buoyancy, consider a penetration depth of 1 foot. The collision force and deceleration would become:

$$F_{\text{collision}} = \frac{(3)(1000 \text{ ft} \cdot \text{lb}_f)}{1 \text{ ft}} = 3.0 \times 10^4 \text{ lb}_f.$$

$$\dot{V}_A = \frac{3.0 \times 10^4 \text{ lb}_f \times g \frac{\text{lb}_m - \text{ft}}{\text{lb}_f - \text{sec}^2}}{15 \text{ L.tons} \times 2240 \frac{\text{lb}_m}{\text{L.ton}}}$$

$$\dot{V}_A = .89g$$

The deceleration just derived is tolerable based on the values given in "General Environmental Requirements For Deep Submersible Vehicles And Submarines" (SAE, April 1969).

(3) A way to reduce the force collision, eliminate the trim moment, maintain present surface buoyancy of 1500 lb_f. and offer protection to station 8, is by using a partially submerged bumper. At station 8, the bumper would be totally submerged. As the bumper proceeds toward the bow, it curves up and above the water line. Finally, at the bow, only a small percent of the bumper remains below the water line. The main surface buoyancy is provided by the portion submerged only. The percent of bumper submerged along the length of the forebody would be determined by trim moment limitations.

The cross-section of the bumper could increase toward the bow. This would allow for greater penetration depths and, thus, lower collision forces in this region. The desired protection perimeter could be obtained by proper selection of the uninflated perimeter. It has been shown earlier that modest increases beyond the present vertical projected area lead to negligible increases in vertical transit time.

By moving the bumper higher-up on ALVIN, the moment arm between the center of gravity and the line of action of the collision force increases. It may be felt that this would increase the tendency for the lower bow region to rotate into the object with which ALVIN is colliding. Since softer bumpers and, therefore, lower collision forces are possible with this system, the rotating moment actually can be reduced. For example, consider the two collision forces determined previously. There was an order of magnitude difference between them. The difference in moment arm between the submerged and surface bumper will be far less than an order of magnitude.

CHAPTER 5
CONCLUSIONS

The purpose of this study was to determine the requirements for an inflatable docking bumper and, specifically, to apply them to DSRV ALVIN. The analysis as shown establishes the following facts:

- (1) With a totally submerged bumper around the bow, there is going to be a problem with trim moment.
- (2) If the uninflated radius is increased in order to increase the protection radius, the trim moment will be increased and vertical transit time will be slightly increased.
- (3) If the displacement is held constant and the protection radius is increased by using all of the available pressure, thereby stiffening the bumper, the collision force and the accompanying decelerations are greatly increased.
- (4) If a totally submerged bumper with a 1500 lb_f. displacement is deemed desirable and the trim moment can be compensated for, collision

forces could be lowered by softening the bumper by not using all of the available pressure in the main air tanks. The desired protection perimeter could be obtained by increasing the uninflated perimeter. This approach sacrifices transit time.

(5) The most feasible design approach appears to be with a partially submerged bumper. This scheme eliminates problems of trim moment, surface buoyancy and collision force. A bonus with the partially submerged bumper is that the view through the forward window in the personnel sphere will not be obstructed by the bumper in either the inflated or uninflated condition. Submerged bumpers would cut-off some of the upper view of the window.

In conclusion, it is felt that inflated bumpers on submersibles are desirable and feasible. Inclusion of the bumper in the original submersible design would eliminate many of the difficulties encountered in trying to design around an existing submersible such as ALVIN.

BIBLIOGRAPHY

- Abkowitz, Martin A. Stability and Motion Control of Ocean Vehicles. Cambridge, Mass.: The M.I.T. Press, 1969.
- Booth, Ronald J.A. Comparative Study of the Heave and Pitch Motions of the Deep Submersible, ALVIN and her Support Catamaran During Surface Operations. Unpublished Technical Memorandum No. DS-24. Woods Hole, Mass.: Woods Hole Oceanographic Institution, 1967.
- Carnahan, B., Luther, H.A., and Wilkes, James O. Applied Numerical Methods. John Wiley and Sons, Inc., New York, 1969.
- Comstock, John P. (ed.). Principles of Naval Architecture. New York: SNAME, 1968.
- "General Environmental Requirements For Deep Submersible Vehicles and Submarines." Society of Automotive Engineers. AIR 1063. (April 15, 1969).
- Hildebrand, F.B. Advanced Calculus for Applications. Prentice-Hall, Inc.: Englewood Cliffs, New Jersey, 1962.
- Hoerner, Sighard F. Fluid Dynamic Drag. Midland Park, N.J.: Published by author, 1965.
- James, R.W., Neumann, G., and Pierson, Jr., W.J. Practical Methods for Observing and Forecasting Ocean Waves by Means of Wave Spectra and Statistics. Washington: U.S. Navy Hydrographic Office, 1955.
- Kenny, James N. A Modeling System for the Dynamics of an Underwater Launch and Recovery of a Deep Submersible. Unpublished Technical Memorandum No. 8-69. Woods Hole, Mass.: Woods Hole Oceanographic Institution, 1969.

Mavor, Jr., J.W., Froehlich, H.E., Marquet, W.M.,
Rannie, W.D. "ALVIN, 6000-Ft. Submergence
Research Vehicle." The Society of Naval Archi-
tects and Marine Engineers. (November 1966).

Newman, J.N. Marine Hydrodynamics. Unpublished
Lecture notes. Cambridge, Mass.: M.I.T.,
1971.

Newman, J.N. "The Damping of an Oscillating Ellipsoid
Near a Free Surface." Journal of Ship Research,
(December 1961).

Vandiver, John K. Dynamic Analysis of a Launch and
Recovery System for a Deep Submersible. Unpub-
lished Manuscript Reference No. 69-88. Woods
Hole, Mass.: Woods Hole Oceanographic Insti-
tution, 1969.